

BRITISH GEOLOGICAL SURVEY

Fluid Processes and Waste Management Group

TECHNICAL REPORT WE/98/49

**VLf surveys on Cyprus:  
Xylophagou, 1998**

David Beamish

*Bibliographic Reference :*  
Beamish D., 1998.  
*VLf Surveys on Cyprus:  
Xylophagou, 1998.*  
British Geological Survey,  
Technical Report, WE/98/49

A report prepared for:  
European Commission  
DG-XII  
Directorate B  
Programme INCO-DC  
75, Rue Montoyer  
B-1040 Brussels



British Geological Survey, Keyworth, Nottingham, 1998

©NERC copyright 1998



## 1) Introduction

This report summarises the results of work undertaken for the EEC INCO-DC project: A new integrated geophysical approach for the rational management and exploration of groundwater resources. The programme Project Number is 950176 under Contract Number ERBIC 18 CT 960122.

EU member participants are:

The Netherlands:	RGD: (NITG-TNO), Haarlem James Baker (Project Coordinator)
France:	BRGM, Orleans Alain Beauce
U.K.:	BGS, Nottingham D. Beamish and Jon Busby

Non-EU partners are:

Cyprus:	GSD, Nicosia Sortiris Kramvis	GEOINVEST, Nicosia Andreas Shiathas
Israel:	GII, Holon Mark Goldman	

This report summarises the field activities of the VLF (Very Low Frequency EM) technique which took place on Cyprus during May and June 1998. Geophysical surveys on Cyprus are designated as Task 3 and the VLF technique designated as sub-task 3.8. VLF fieldwork took place mainly along a main N-S profile in the Xylofagou area of eastern Cyprus. VLF observations along more limited traverses also took place at a few selected localities on the pillow lavas in the Troodos area. This report describes only the VLF survey in the Xylofagou area.

## 2) The VLF technique

The VLF survey technique is a well-established electromagnetic (EM) method of applied geophysics. McNeill and Labson (1991) review its use for geological and hydrogeological applications. The method is one of a class of EM techniques that conform to a plane-wave sounding of subsurface resistivity structure; a closely allied (natural-field) technique is the audiomagnetotelluric (AMT) method (e.g. Strangway et al., 1973). The VLF-EM technique makes use of one or more distant radio transmitters operating between 15 and 30 kHz. The limited bandwidth means that, although several measurements may be obtained at different frequencies (using different transmitters), a main attribute of the method is that of a single frequency sounding. The fact that the instrumentation is very portable and cost-effective survey method compensate for the lack of bandwidth. The VLF method was developed as an inductive

sounding technique measuring the amplitude and (subsequently) phase relationship between the vertical (secondary) magnetic field (Z) relative to the horizontal primary field (H). This method, referred to here as VLF-Z, relies on wavefield interaction with two-dimensional (2-D) and three-dimensional (3-D) resistivity structure. The technique has since been extended to include a measure of the induced horizontal electric field (E) component. This VLF-R measurement provides an impedance value (e.g. E/H), usually expressed as apparent resistivity and phase, using short (e.g. 5 m) electric dipoles. The VLF-R measurement, although appropriate for a one-dimensional (1-D) application, contains only marginal information on the vertical resistivity structure (Fischer et al., 1983) because, in effect, only a single frequency is available. These factors suggest that the strength of VLF methods lie predominantly in the definition of lateral gradients in the subsurface resistivity structure. The interpretation problem is therefore, at least, two-dimensional.

As discussed by Fischer et al. (1983) and Beamish (1998), in order to ensure consistency with a 2-D approach, the directional VLF data must conform to one of the two principal modes of 2-D induction. The assumption of infinite strike (which defines the 2-D case) provides two decoupled modes involving separate combinations of the field components. The TE-mode (or E-polarisation, electric field parallel to strike) involves surface fields of  $E_x$ ,  $H_y$  and  $H_z$ . The TM-mode (or H-polarisation, magnetic field parallel to strike) involves the surface fields  $H_x$ ,  $E_y$  and  $E_z$ .

Due to the directional nature of VLF measurements, we require therefore that the measurements be made in, at least one, of the two principal directions. Where the geological strike is not known, the sensible survey option of taking measurements from several azimuthally distinct transmitters may be used.

### 3) Cyprus Field Work

#### 3.1 Xylophagou Field Area

The hydrogeology of the field area is described in an unpublished report prepared for the fieldwork by Geoinvest Ltd. The report describes the main Kokkinokhoria aquifer as the major and most productive part of the general SE Mesaoria aquifer and provides details of its overexploitation. A secondary limestone crust (Kafkalla) and deep red soils tend to obscure the surface features of the area. Four main aquiferous units are recognised: (a) the sandy aquifer, made up of the upper sandy section of a Plio-Pleistocene sequence extending throughout the SE Mesaoria, (b) the limestone aquifer of the Miocene reef limestone facies which is in contact with the sandy aquifer, (c) the gypsum aquifer at the top of the Middle Miocene sequence containing highly saline water and (d) the chalk aquifer of the Palaeocene – Lower Miocene sequence.

The aquifer tends to be compartmentalised in a series of vertical faults. A normal E-W fault, south of Xylophagou, separates the Cape Pyla horst, mainly of reef limestone, from the aquifer. Figure 3.1 shows the field area and an initial location map of the main N-S geophysical traverse. The profile origin is located in the south and the traverse crosses the main reef limestone. Boreholes GR33 (to the west of the profile), 30/40 (close to the profile) and 92/52 (to the east of the profile) can be used as control. The borehole log of GR33 has a depth of 222.5 m and indicates chalk and marly chalk to a depth of 15 m, below this depth the log records a crystalline

porous and cavernous dolomitic and reef limestone. Borehole 30/40 is 300 m east of the traverse (1600 m along the line) and the log records 44.2 m of limestone. The borehole log of 92/52 records 21 m of hard white limestone.

### 3.2 VLF data acquisition

VLF data collection took place between May 30 and June 08 1998. The measurements were made with the Scintrex IGS-2 equipment, using 5 metre, capacitively-coupled E-field dipoles. The equipment has a reading resolution of 1% in the case of the VLF-Z components and 1 ohm.m and 1 degree in the case of the VLF-R measurements.

A systematic study of VLF horizontal magnetic field signal strengths was conducted across the bandwidth from 15 to 30 kHz. In contrast to Western Europe, all transmissions on Cyprus were found to be weak and often close-to or below the noise level of the instrument. Transmissions providing a N-S E-field were a particular problem. The strongest N-S transmissions were found at frequencies of 18.0, 18.1 and 23.5 kHz. In practice, all the N-S signals were found to be intermittent. The most reliable and strong VLF transmission providing an E-W E-field was the 18.3 kHz transmission (HWE, Le Blanc, France). This frequency was used extensively during the survey.

Skin-depths at 18.3 kHz range from 11.8 m (in 10 ohm.m material), to 26.3 m (in 50 ohm.m material) through to 37.2 m (in 100 ohm.m) material. VLF penetration depths, in uniform materials, are a factor of 1.5 greater than the skin-depth.

## 4) Data for the Xylofagou profile

VLF data were collected at 5 m intervals along the main N-S geophysical traverse that ran from near the coast (i.e. towards the profile origin) in the south and northwards (inland). VLF data were collected along the profile from 100 m through to 2100 m. The data were collected over several days. In each case attempts were made to collect VLF-R and VLF-Z using two orthogonal (N-S and E-W) transmitters. The only reliable transmissions were those at 18.3 KHz, which were measured using E-W electric field dipoles. As a consequence the only continuous (i.e. every 5 m) data set was obtained using the E-W 18.3 kHz signal.

The complete VLF-Z set for the Xylofagou profile is shown in Figure 4.1 from 100 to 2100 m. Despite the fact that high-wavenumber noise is apparent at the data sampling interval, significant longer wavelength features can be observed in both real and imaginary components. There appears to be a transition at 400-500 m along the profile. In general, the real response is largely negative while the imaginary response is only slightly positive.

The corresponding VLF-R data set along the profile is shown in Figure 4.2. A logarithmic scale for apparent resistivity has been used due to the large range of values encountered (from  $< 10$  to  $> 1000$  ohm.m). In broad terms, the majority of apparent resistivity values lie in the range 10 to 100 ohm.m while the phase values are generally  $> 45$  degrees. Again, despite the fact that high-wavenumber noise is apparent at the data sampling interval, significant longer wavelength features can be observed in both amplitude and phase values.

In order to extract reliable information at a regional scale across the profile, the raw data shown in Figures 4.1 and 4.2 have been low-pass filtered. A finite-impulse response filter with a low cut point at 50 m was designed and applied to the two data sets. The raw and low-pass filtered data are shown in Figures 4.3 (VLF-Z) and 4.4 (VLF-R).

The filtered data set comprises 201 data points resampled every 10 m, between 100 and 2100 m. These data have been used to investigate the resistivity distribution along the traverse.

## 5) 2D regularised inversion of VLF data

### 5.1 Theory

The starting point in the modelling of VLF data are the developments in non-linear inversion which have arisen in the context of the multi-frequency MT technique. The new approaches involve regularising an otherwise 'ill-posed' problem by introducing a smooth or minimum-structure constraint. In 2-D inversion, the problem of equivalence becomes particularly acute because of the larger number of degrees of freedom within the model space. The essential point is that the minimum-structure inversion concept acknowledges this fact and allows the construction of credible (non-extreme) resistivity models.

For 2-D MT inversion, deGroot-Hedlin and Constable (1990) implemented a minimum-structure inversion which is referred to as OCCAM and is based on the finite-element forward solution of Wannamaker et al. (1987). A more rapid 2D inversion code involving a non-linear, conjugate gradient (NLCG) algorithm has recently been described by Rodi and Mackie (1998). The algorithm implements first-derivative smoothing and includes a regularisation parameter ( $\tau$ ) that controls the degree of model smoothness/roughness (often a trade-off with misfit). VLF studies using the former method were described by Beamish (1994). The latter method is used in the present study since it readily permits the use of a regular subsurface finite-difference grid comprising in excess of 100x100 1 m cells. A limitation of the present algorithm is that joint inversion of VLF-R and VLF-Z data is not yet installed.

The measured data should possess error bounds. An *exact* fit between measured and modelled data is rarely warranted. The error bound must comprise the variance associated with physical measurement but it can also encompass the degree to which a particular level of modelling (e.g. 1D, 2D or 3D) is thought to be appropriate. Given a set of N observations ( $o_i$ ,  $i=1,N$ ) with standard errors ( $\sigma_i$ ), the concept is to only fit the observations to within a prescribed level of misfit. When the data and errors conform to Gaussian behaviour the chi-square ( $\chi^2$ ) statistic is a natural measure of misfit :

$$\chi^2 = \sum (o_i - m_i)^2 / \sigma_i^2$$

where  $m_i$  refers to the  $i$ 'th model response. An r.m.s. measure of misfit defined as  $\chi^2/N$  with an expectation value of unity is used here.

## 5.2) Application to field data

In order to implement the data inversion, it is assumed that the survey data, collected with the E-field in an E-W direction, conform to a TE-mode response. This is a realistic assumption in view of the related behaviour of both VLF-R and VLF-Z data (a pure TM-mode response does not produce a VLF-Z response). The assessment of structure along the Xylophagou profile is in terms of E-W striking resistivity variations.

A subsurface model grid comprising 201 10 m elements in the horizontal direction and 20 1 m elements in the vertical direction was developed. Beyond this central section, the grid expands to meet uniform boundary condition requirements. Below a depth of 20 m, the grid elements increase to 2, 3, 5 and 10 m thicknesses. The inversion was initiated using a half-space value of 250 ohm.m. A smoothing parameter of 3 was employed (Rodi and Mackie, 1998). Nominal data error assignments of 10% were applied to both apparent resistivity and phase data.

Inversion of the data resulted in an rms misfit of 1.5% (under the assumption of 10%) error bounds. A comparison of observed and modelled data is shown in Figure 5.1. It can be seen that all the main observed variations are adequately modelled. The resistivity model along the 2 km profile is shown in Figure 5.2 at a vertical exaggeration of x20. The colour-bar scale of resistivities is arranged to show high resistivities (100 to 1000 ohm.m and > 1000 ohm.m) which are taken to represent regions of highly intact limestone. Moderate resistivities (10 to 100 ohm.m) appear to represent the main 'background' resistivity along the profile. Several regions of very low resistivities are imaged. The main low resistivity region with an undulating upper surface (10 to 20 m deep) is located between 1400 and 1800 m. It is assumed that the low resistivity zones arise due to an increase in fracture intensity.

The resistivity distribution shown in Figure 5.2 is highly vertically exaggerated. The lateral configuration of the resistivity distribution is likely to be well resolved. The vertical extent of the zones is probably less well resolved. Due to the wide range of resistivities encountered, the maximum depth of the model shown in Figure 5.2 is unrealistic across the whole length of the profile.

In order to show the resistivity distribution at a more realistic scale, a portion of the model between 1400 and 1600 m, where the low resistivity zone is present, is shown at a vertical exaggeration of x2 in Figure 5.3. Along this section of the profile, resistivities in excess of 100 ohm.m are only associated with a small portion of the near-surface.

## 6) Summary

A 2 km profile of VLF data was acquired along a main N-S geophysical line crossing the Cape Pyla reef limestone. Both VLF-R and VLF-Z data were acquired. Attempts were made to obtain data from both N-S and E-W VLF transmissions. Due to poor signal strengths from N-S transmitters, only the E-W (E-field) transmissions of the HWE transmitter at a frequency of 18.3 kHz proved reliable.

Both VLF-R and VLF-Z 18.3 kHz data were acquired at 5 m intervals, with an E-W E-field, along the main profile from 100 to 2100 m. High wavenumber noise at the measurement scale is

apparent in both the VLF-R and VLF-Z data. Such noise is likely to be geological in origin and may be introduced by small-scale irregularities associated with near-surface features in the partially-exposed limestone crust (Kafkalla). In order to provide a regionally representative data set the raw data have been low-pass filtered.

The VLF-R data indicate a wide range of resistivities from 10 to over 1000 ohm.m. Both the VLF-R and VLF-Z data indicate a high degree of lateral resistivity variation across the profile. The joint behaviour of the VLF-R and VLF-Z data indicate that the response observed is a TE-mode responding primarily to E-W structural variations.

The VLF-R data, resampled at an interval of 10 m, have been inverted using a new NLCCG algorithm. The response of the resulting resistivity model has an rms misfit of 1.6% when 10% observational errors are assumed. The resistivity model presented has regions of high resistivity (e.g. 100 to 1000 ohm.m and > 1000 ohm.m) both at shallow depths (< 10 m) and in vertical zones. These zones are tentatively taken to represent zones of highly intact limestone. Moderate resistivities (10 to 100 ohm.m) appear to represent the main 'background' resistivity along the profile. Several regions of very low resistivities (< 10 ohm.m) are imaged. The main low resistivity region with an undulating upper surface (10 to 20 m deep) is located between 1400 and 1800 m. It is assumed that the low resistivity zones arise due to an increase in fracture intensity.

## 7) References

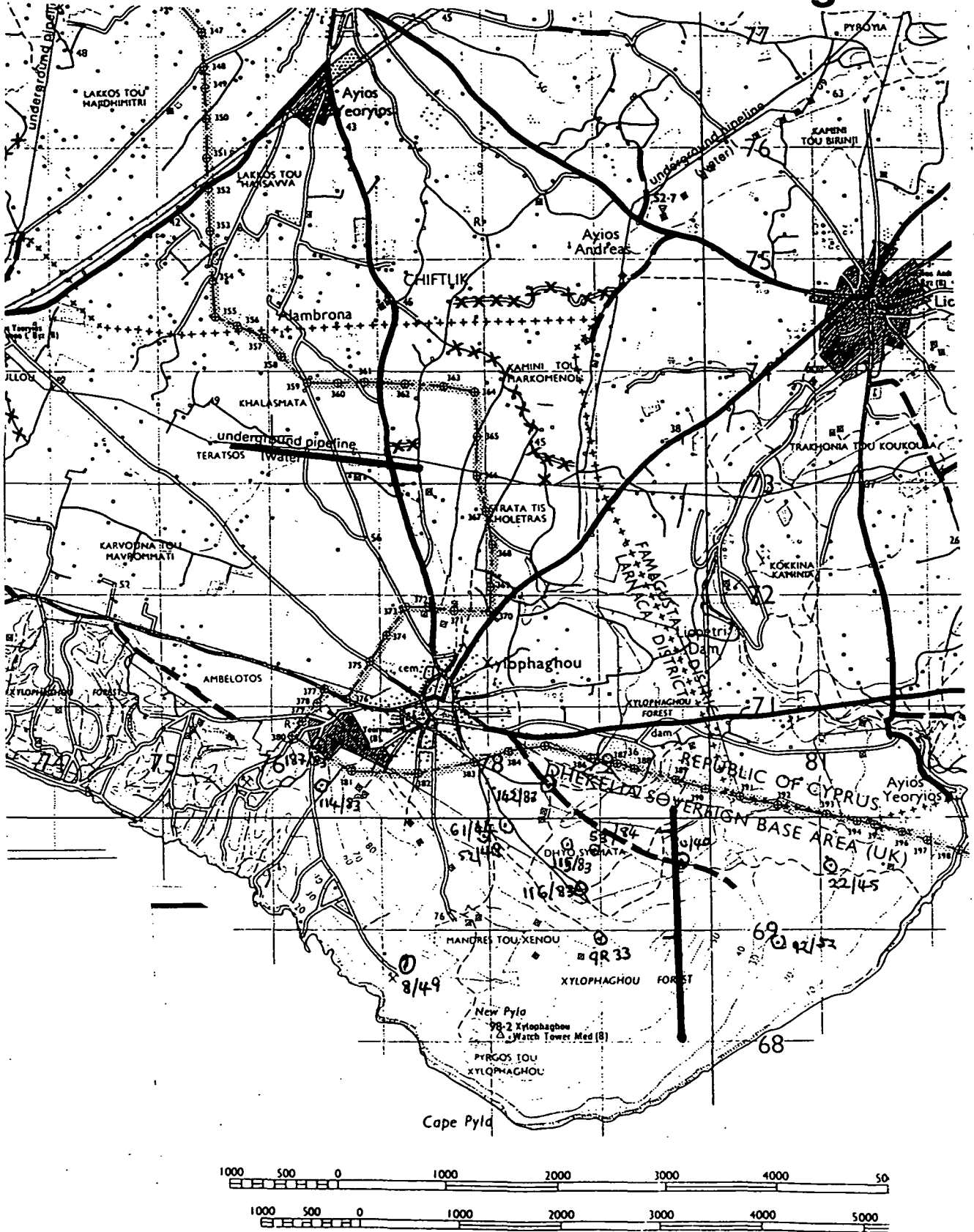
- Beamish, D., 1994. Two-dimensional, regularised inversion of VLF data. *Journal of Applied Geophysics*, 32, 357-374.
- Beamish, D., 1998. Three-dimensional modelling of VLF data. *J. Applied Geophysics*, 39, 63-76.
- deGroot-Hedlin, C.M. and Constable, S.C., 1990. Occam's inversion to generate smooth, two-dimensional models from magnetotelluric data. *Geophysics*, 55: 1613-1624.
- Fischer, G., Le Quang, B.V. and Muller, I., 1983. VLF ground surveys, a powerful tool for the study of shallow two-dimensional structures. *Geophys. Prosp.*, 31: 977-991.
- McNeill, J.D. and Labson, V.F., 1991. Geological mapping using VLF radio fields. In: Nabighian, M. (Editor), *Electromagnetic Methods in Applied Geophysics, Part B: Application*. SEG, Tulsa, pp. 521-640.
- Rodi, W. and Mackie, R.L., 1998. Nonlinear conjugate gradients algorithm for 2-D magnetotelluric inversion, *Geophysics*, submitted.
- Strangway, D.W., Swift, Jr, C.M. and Holmer, R.C., 1973. The application of audio-frequency magnetotellurics (AMT) to mineral exploration. *Geophysics*, 38: 1159-1175.
- Tabbagh, A., Benderitter, Y., Andrieux, P., Decriaud, J.P. and Guerin, R., 1991. VLF resistivity mapping and verticalization of the electric field. *Geophys. Prosp.*, 39: 1083-1097.

Wannamaker, P.E., Stodt, J.A. and Rijo, L., 1987. A stable finite element solution for two-dimensional magnetotelluric modelling. *Geophys. J. R. astr. Soc.*, **88**: 277-296.

## **8) Acknowledgements**

It is a pleasure to acknowledge the major contribution made by the GSD, Nicosia during the field work. Many members of staff were involved and I thank them all.

Fig. 3.1

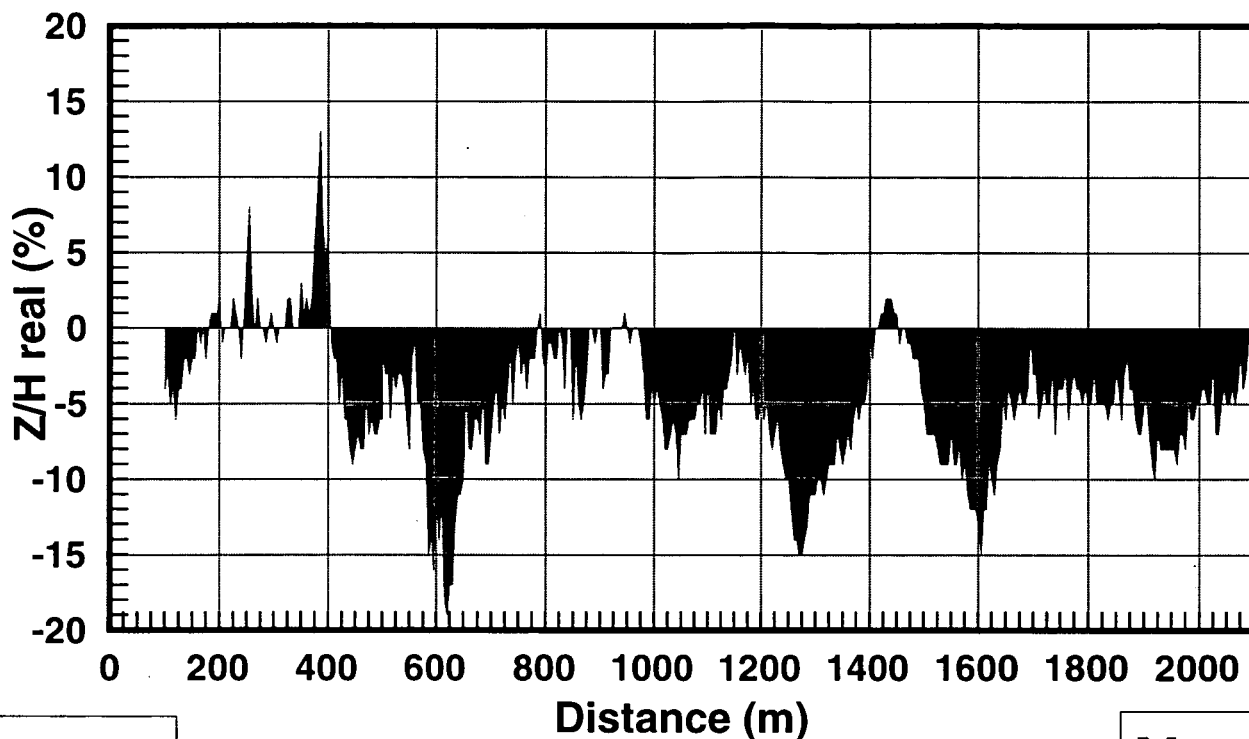


**Xylophagou VLF survey location (provisional)**

Fig. 4.1

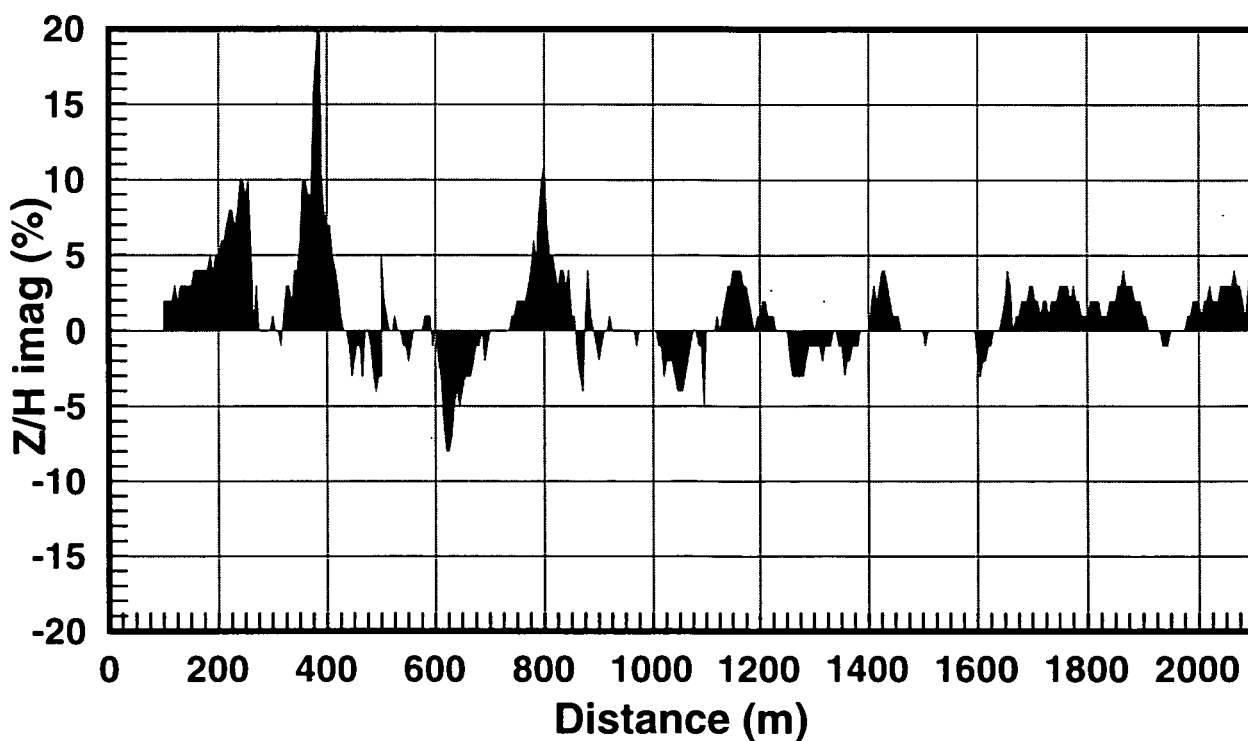
**Xylophagu VLF survey 1998**

**18.3 kHz E-W 5m interval**



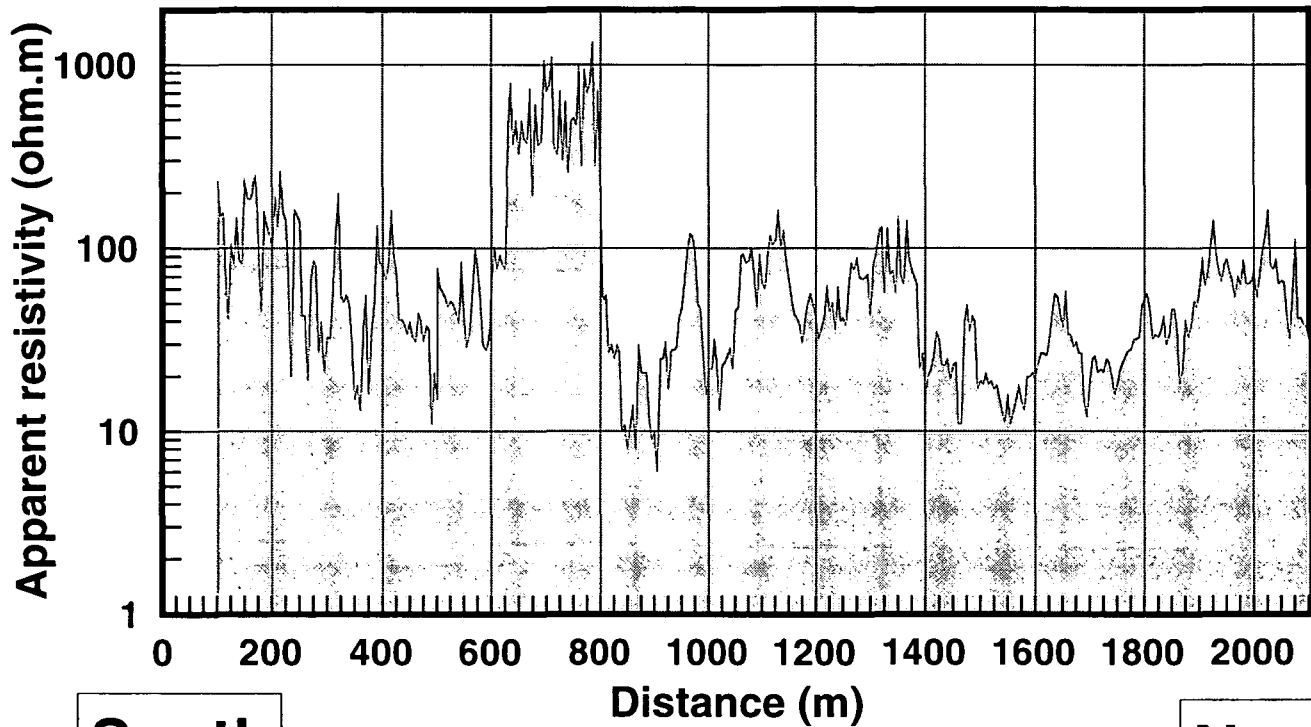
**South**

**North**



**Xylophagu VLF survey 1998**

**18.3 kHz E-W 5m interval**



**South**

**North**

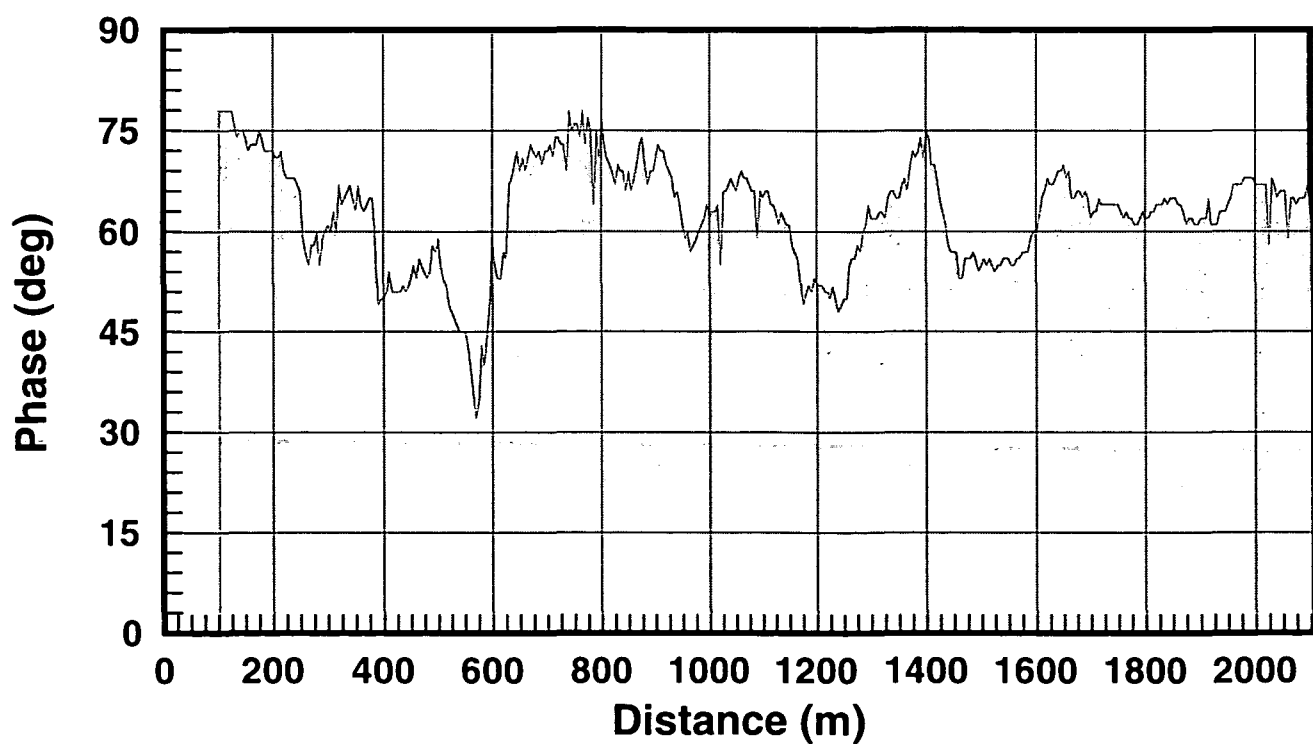


Fig. 4.3

**Xylophagu VLF survey 1998**

**18.3 kHz E-W 5m interval, 50 m LP**

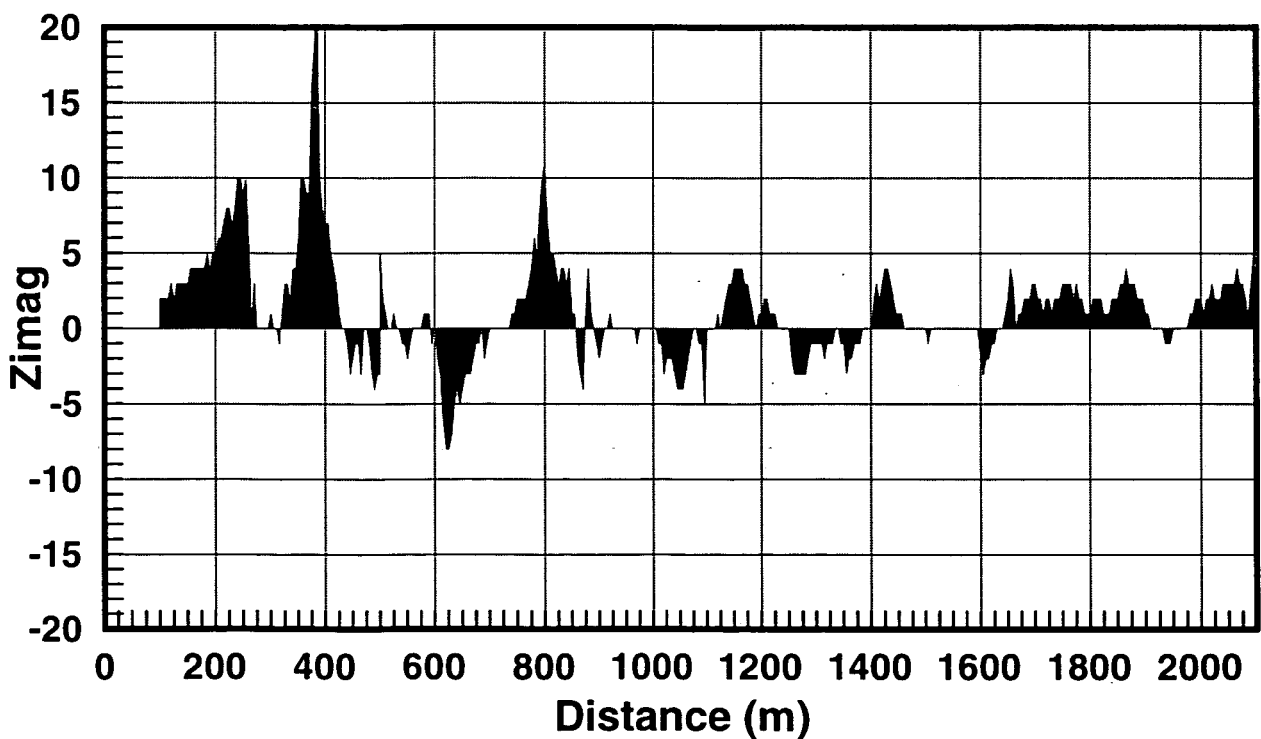
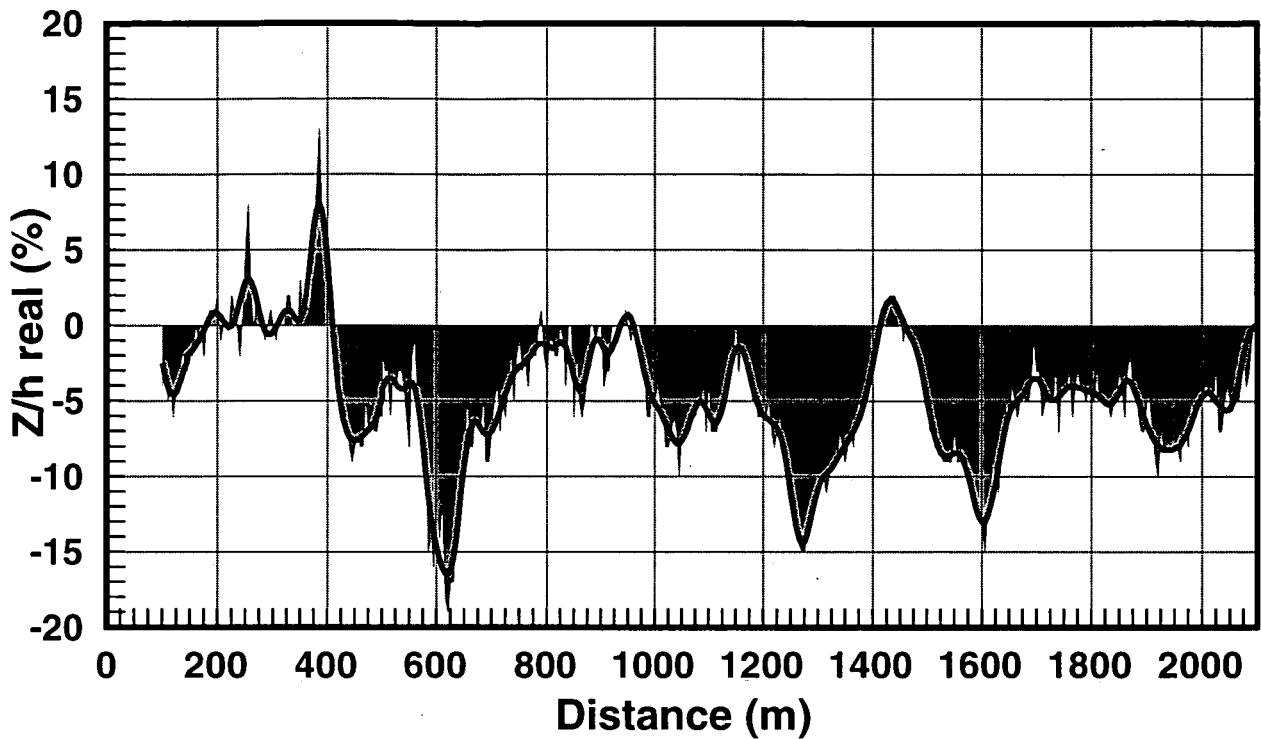
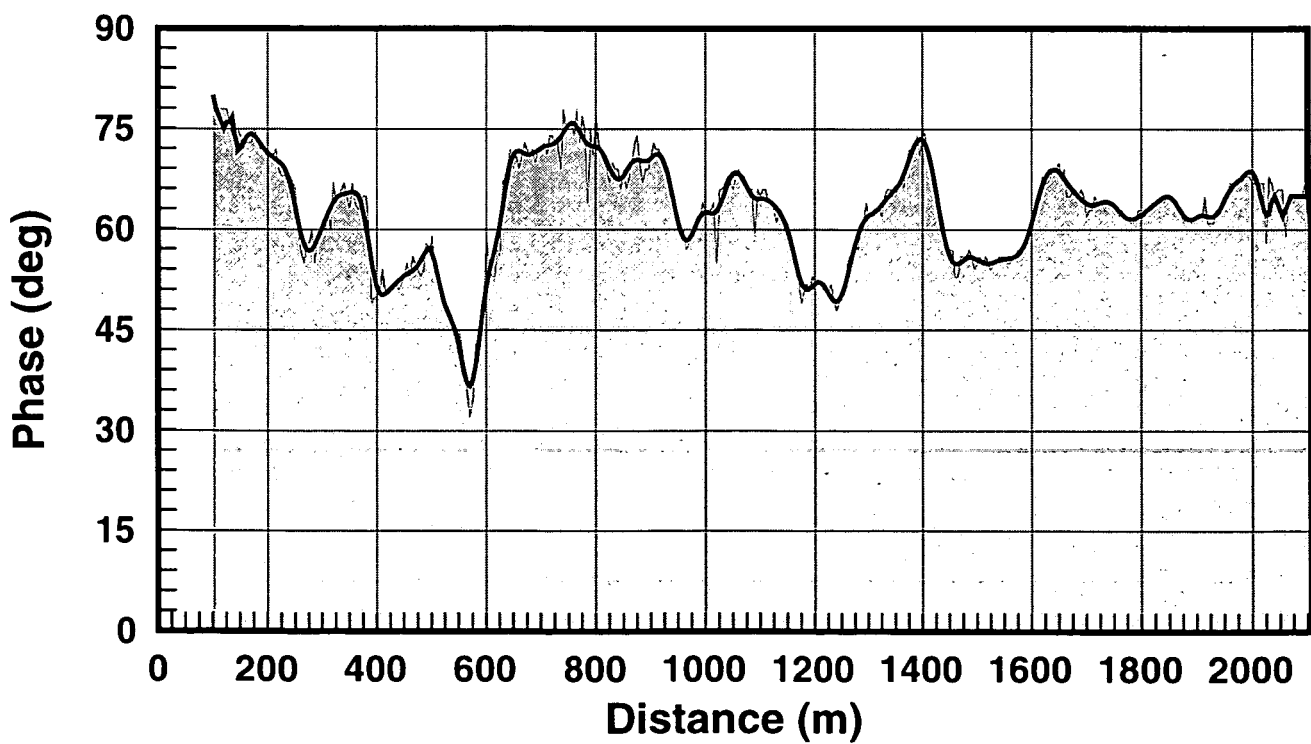
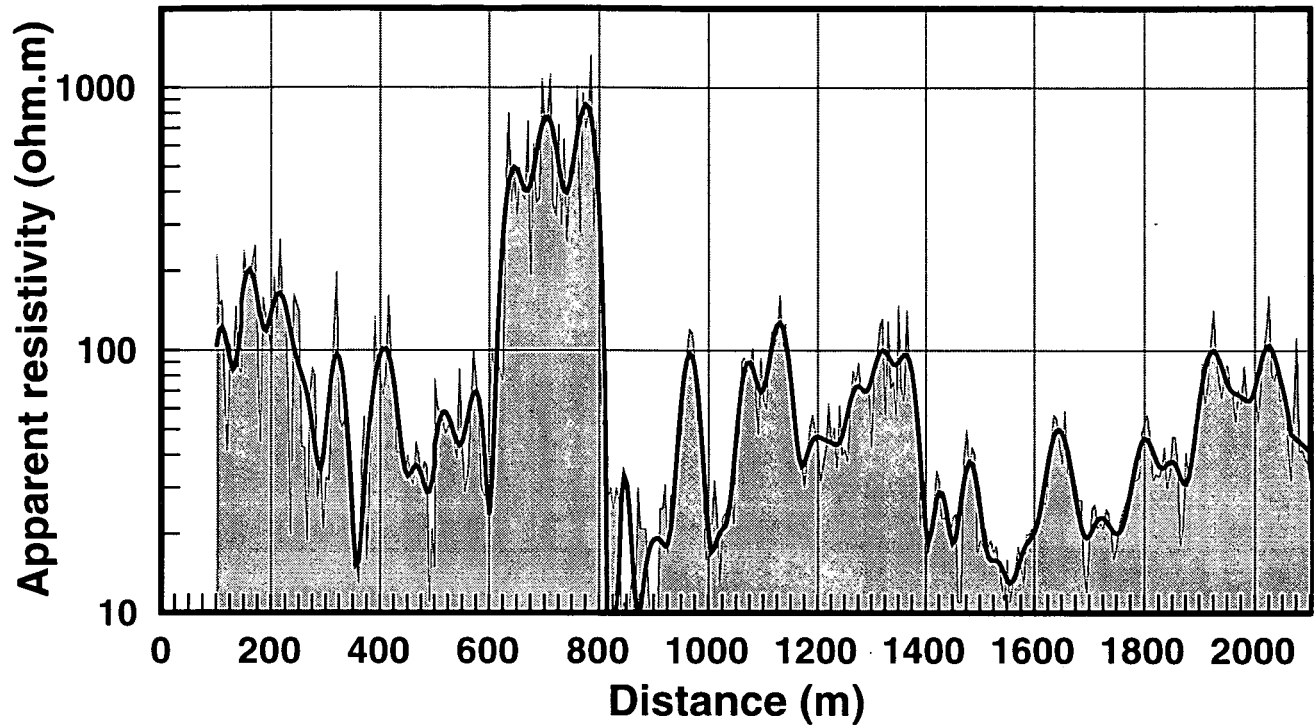


Fig. 4.4

**Xylophagu VLF survey 1998**

**18.3 kHz E-W 5m interval, 50 m LP**

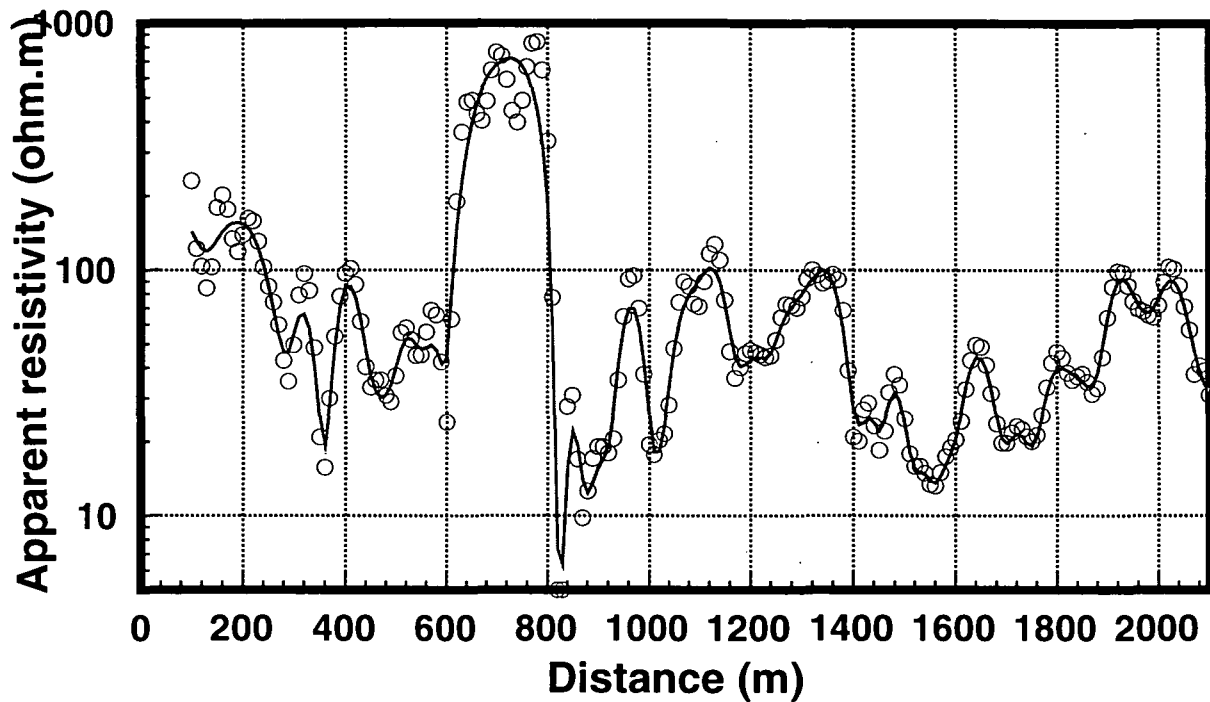


# Xylophagu VLF survey 1998

18.3 kHz E-W 10 m interval

Comparison of observed and modelled results

TE-mode. 2d NLCG. 10% data errors gives rms misfit of 1.5%



South

North

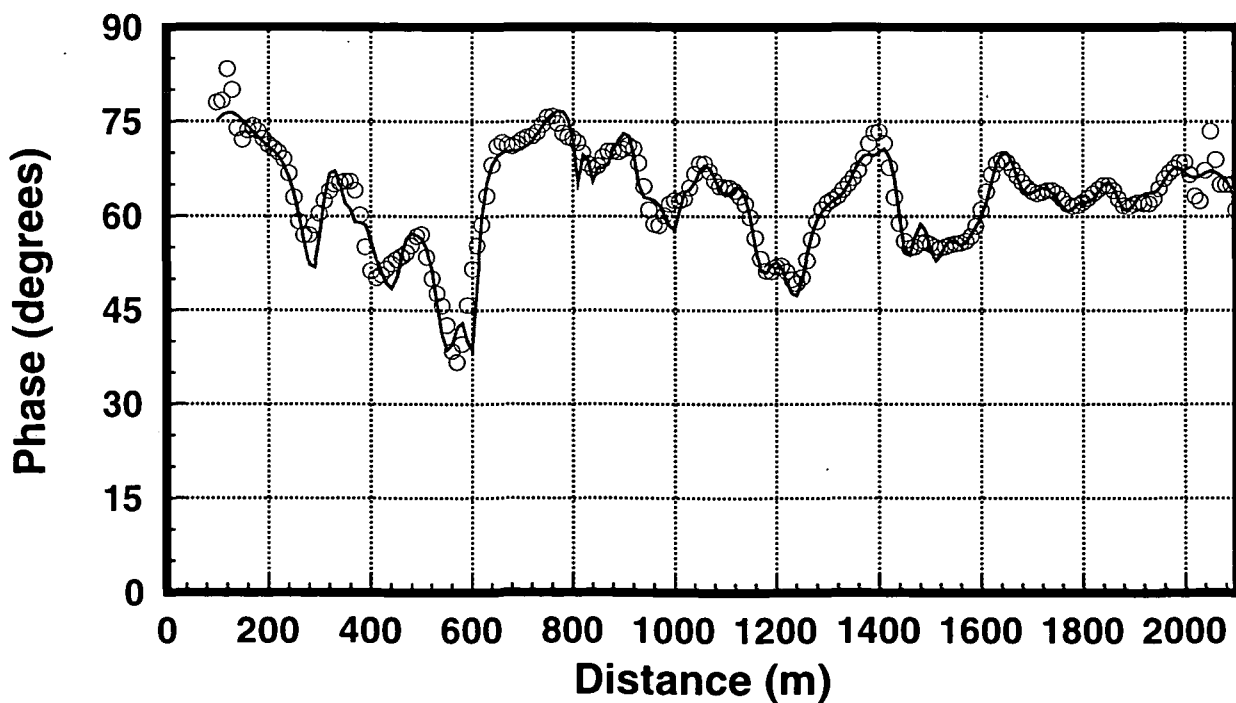
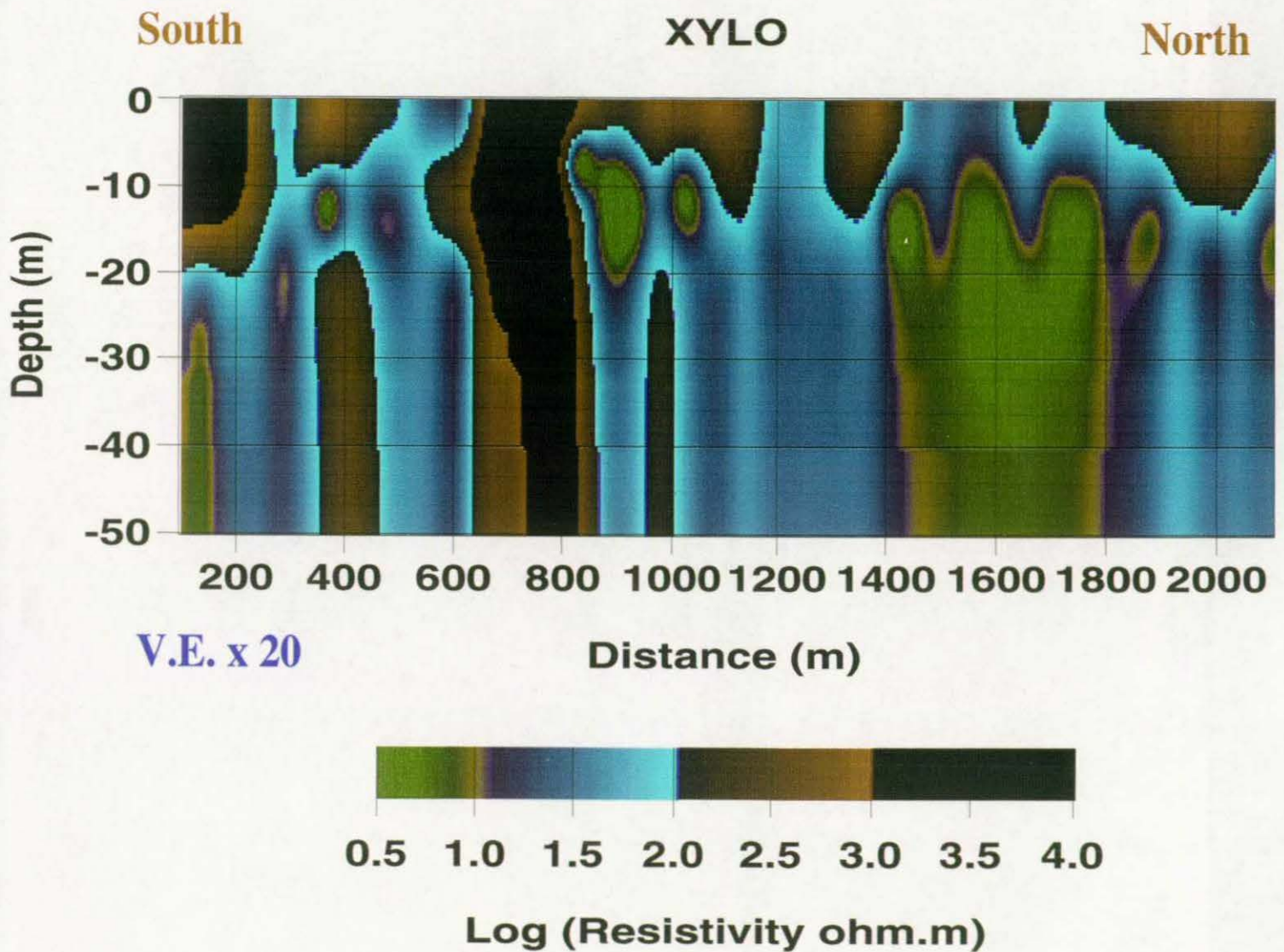


**Fig. 5.2**

**Cyprus VLF survey 98**

**Xylophagu 18.3 kHz TE**

**2D resistivity model using NLCG inversion**



TE-mode. 2d bNLCG. 10% data errors give misfit of 1.6%

Filtered data at 10 m, 201 observations of apparent resistivity and phase

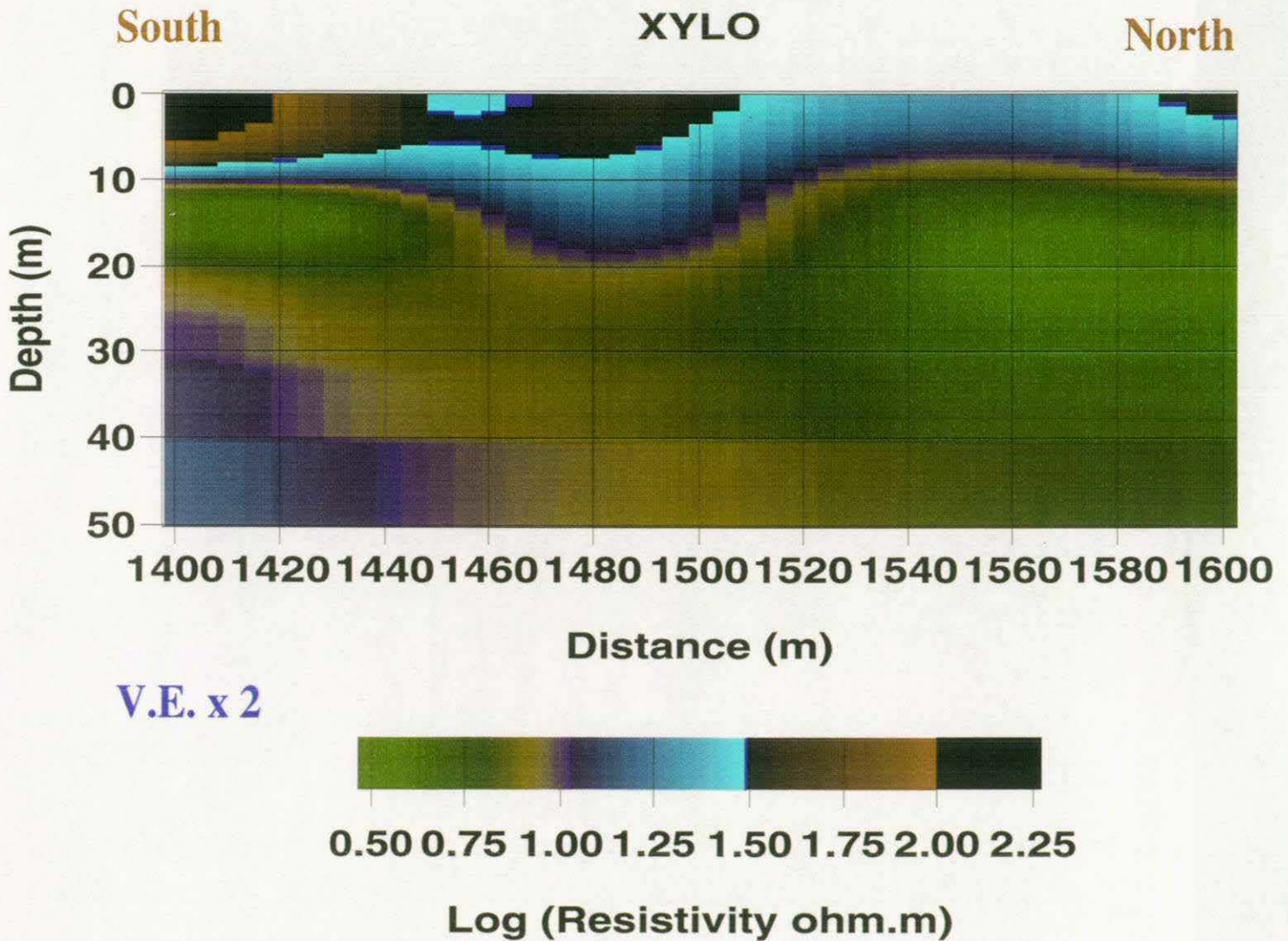
**Fig. 5.3**

**Cyprus VLF survey 98**

**Xylophagu 18.3 kHz TE**

**2D resistivity model using NLCG inversion**

**200 m detail from model**



TE-mode. 2d bNLCG. 10% data errors give misfit of 1.6%

Filtered data at 10 m, 201 observations of apparent resistivity and phase

BRITISH GEOLOGICAL SURVEY

Fluid Processes and Waste Management Group

TECHNICAL REPORT WE/98/49

**VLF surveys on Cyprus:  
Xylophagou, 1998**

David Beamish

*Bibliographic Reference :*  
Beamish D., 1998.  
*VLF Surveys on Cyprus:  
Xylophagou, 1998.*  
British Geological Survey,  
Technical Report, WE/98/49

A report prepared for:  
European Commission  
DG-XII  
Directorate B  
Programme INCO-DC  
75, Rue Montoyer  
B-1040 Brussels



British Geological Survey, Keyworth, Nottingham, 1998

©NERC copyright 1998



## CONTENTS

<b>1) Introduction</b>	<b>2</b>
<b>2) The VLF Technique</b>	<b>2</b>
<b>3) Cyprus Field Work</b>	<b>3</b>
<b>3.1 Xylophagou Field Area</b>	<b>3</b>
<b>3.2 VLF data acquisition</b>	<b>4</b>
<b>4) Data for the Xylofagou profile</b>	<b>4</b>
<b>5) 2D regularised inversion of VLF data</b>	<b>5</b>
<b>5.1 Theory</b>	<b>5</b>
<b>5.2) Application to field data</b>	<b>6</b>
<b>6) Summary</b>	<b>6</b>
<b>7) References</b>	<b>7</b>
<b>8) Acknowledgements</b>	<b>8</b>

---

## 1) Introduction

This report summarises the results of work undertaken for the EEC INCO-DC project: A new integrated geophysical approach for the rational management and exploration of groundwater resources. The programme Project Number is 950176 under Contract Number ERBIC 18 CT 960122.

EU member participants are:

The Netherlands:	RGD: (NITG-TNO), Haarlem James Baker (Project Coordinator)	
France:	BRGM, Orleans Alain Beauce	
U.K.:	BGS, Nottingham D. Beamish and Jon Busby	

Non-EU partners are:

Cyprus:	GSD, Nicosia Sortiris Kramvis	GEOINVEST, Nicosia Andreas Shiathas
Israel:	GII, Holon Mark Goldman	

This report summarises the field activities of the VLF (Very Low Frequency EM) technique which took place on Cyprus during May and June 1998. Geophysical surveys on Cyprus are designated as Task 3 and the VLF technique designated as sub-task 3.8. VLF fieldwork took place mainly along a main N-S profile in the Xylofagou area of eastern Cyprus. VLF observations along more limited traverses also took place at a few selected localities on the pillow lavas in the Troodos area. This report describes only the VLF survey in the Xylofagou area.

## 2) The VLF technique

The VLF survey technique is a well-established electromagnetic (EM) method of applied geophysics. McNeill and Labson (1991) review its use for geological and hydrogeological applications. The method is one of a class of EM techniques that conform to a plane-wave sounding of subsurface resistivity structure; a closely allied (natural-field) technique is the audiomagnetotelluric (AMT) method (e.g. Strangway et al., 1973). The VLF-EM technique makes use of one or more distant radio transmitters operating between 15 and 30 kHz. The limited bandwidth means that, although several measurements may be obtained at different frequencies (using different transmitters), a main attribute of the method is that of a single frequency sounding. The fact that the instrumentation is very portable and cost-effective survey method compensate for the lack of bandwidth. The VLF method was developed as an inductive

sounding technique measuring the amplitude and (subsequently) phase relationship between the vertical (secondary) magnetic field (Z) relative to the horizontal primary field (H). This method, referred to here as VLF-Z, relies on wavefield interaction with two-dimensional (2-D) and three-dimensional (3-D) resistivity structure. The technique has since been extended to include a measure of the induced horizontal electric field (E) component. This VLF-R measurement provides an impedance value (e.g. E/H), usually expressed as apparent resistivity and phase, using short (e.g. 5 m) electric dipoles. The VLF-R measurement, although appropriate for a one-dimensional (1-D) application, contains only marginal information on the vertical resistivity structure (Fischer et al., 1983) because, in effect, only a single frequency is available. These factors suggest that the strength of VLF methods lie predominantly in the definition of lateral gradients in the subsurface resistivity structure. The interpretation problem is therefore, at least, two-dimensional.

As discussed by Fischer et al. (1983) and Beamish (1998), in order to ensure consistency with a 2-D approach, the directional VLF data must conform to one of the two principal modes of 2-D induction. The assumption of infinite strike (which defines the 2-D case) provides two decoupled modes involving separate combinations of the field components. The TE-mode (or E-polarisation, electric field parallel to strike) involves surface fields of  $E_x$ ,  $H_y$  and  $H_z$ . The TM-mode (or H-polarisation, magnetic field parallel to strike) involves the surface fields  $H_x$ ,  $E_y$  and  $E_z$ .

Due to the directional nature of VLF measurements, we require therefore that the measurements be made in, at least one, of the two principal directions. Where the geological strike is not known, the sensible survey option of taking measurements from several azimuthally distinct transmitters may be used.

### 3) Cyprus Field Work

#### 3.1 Xylophagou Field Area

The hydrogeology of the field area is described in an unpublished report prepared for the fieldwork by Geoinvest Ltd. The report describes the main Kokkinokhoria aquifer as the major and most productive part of the general SE Mesaoria aquifer and provides details of its overexploitation. A secondary limestone crust (Kafkalla) and deep red soils tend to obscure the surface features of the area. Four main aquiferous units are recognised: (a) the sandy aquifer, made up of the upper sandy section of a Plio-Pleistocene sequence extending throughout the SE Mesaoria, (b) the limestone aquifer of the Miocene reef limestone facies which is in contact with the sandy aquifer, (c) the gypsum aquifer at the top of the Middle Miocene sequence containing highly saline water and (d) the chalk aquifer of the Palaeocene – Lower Miocene sequence.

The aquifer tends to be compartmentalised in a series of vertical faults. A normal E-W fault, south of Xylophagou, separates the Cape Pyla horst, mainly of reef limestone, from the aquifer. Figure 3.1 shows the field area and an initial location map of the main N-S geophysical traverse. The profile origin is located in the south and the traverse crosses the main reef limestone. Boreholes GR33 (to the west of the profile), 30/40 (close to the profile) and 92/52 (to the east of the profile) can be used as control. The borehole log of GR33 has a depth of 222.5 m and indicates chalk and marly chalk to a depth of 15 m, below this depth the log records a crystalline

porous and cavernous dolomitic and reef limestone. Borehole 30/40 is 300 m east of the traverse (1600 m along the line) and the log records 44.2 m of limestone. The borehole log of 92/52 records 21 m of hard white limestone.

### 3.2 VLF data acquisition

VLF data collection took place between May 30 and June 08 1998. The measurements were made with the Scintrex IGS-2 equipment, using 5 metre, capacitively-coupled E-field dipoles. The equipment has a reading resolution of 1% in the case of the VLF-Z components and 1 ohm.m and 1 degree in the case of the VLF-R measurements.

A systematic study of VLF horizontal magnetic field signal strengths was conducted across the bandwidth from 15 to 30 kHz. In contrast to Western Europe, all transmissions on Cyprus were found to be weak and often close-to or below the noise level of the instrument. Transmissions providing a N-S E-field were a particular problem. The strongest N-S transmissions were found at frequencies of 18.0, 18.1 and 23.5 kHz. In practice, all the N-S signals were found to be intermittent. The most reliable and strong VLF transmission providing an E-W E-field was the 18.3 kHz transmission (HWE, Le Blanc, France). This frequency was used extensively during the survey.

Skin-depths at 18.3 kHz range from 11.8 m (in 10 ohm.m material), to 26.3 m (in 50 ohm.m material) through to 37.2 m (in 100 ohm.m) material. VLF penetration depths, in uniform materials, are a factor of 1.5 greater than the skin-depth.

## 4) Data for the Xylofagou profile

VLF data were collected at 5 m intervals along the main N-S geophysical traverse that ran from near the coast (i.e. towards the profile origin) in the south and northwards (inland). VLF data were collected along the profile from 100 m through to 2100 m. The data were collected over several days. In each case attempts were made to collect VLF-R and VLF-Z using two orthogonal (N-S and E-W) transmitters. The only reliable transmissions were those at 18.3 KHz, which were measured using E-W electric field dipoles. As a consequence the only continuous (i.e. every 5 m) data set was obtained using the E-W 18.3 kHz signal.

The complete VLF-Z set for the Xylofagou profile is shown in Figure 4.1 from 100 to 2100 m. Despite the fact that high-wavenumber noise is apparent at the data sampling interval, significant longer wavelength features can be observed in both real and imaginary components. There appears to be a transition at 400-500 m along the profile. In general, the real response is largely negative while the imaginary response is only slightly positive.

The corresponding VLF-R data set along the profile is shown in Figure 4.2. A logarithmic scale for apparent resistivity has been used due to the large range of values encountered (from < 10 to > 1000 ohm.m). In broad terms, the majority of apparent resistivity values lie in the range 10 to 100 ohm.m while the phase values are generally > 45 degrees. Again, despite the fact that high-wavenumber noise is apparent at the data sampling interval, significant longer wavelength features can be observed in both amplitude and phase values.

In order to extract reliable information at a regional scale across the profile, the raw data shown in Figures 4.1 and 4.2 have been low-pass filtered. A finite-impulse response filter with a low cut point at 50 m was designed and applied to the two data sets. The raw and low-pass filtered data are shown in Figures 4.3 (VLF-Z) and 4.4 (VLF-R).

The filtered data set comprises 201 data points resampled every 10 m, between 100 and 2100 m. These data have been used to investigate the resistivity distribution along the traverse.

## 5) 2D regularised inversion of VLF data

### 5.1 Theory

The starting point in the modelling of VLF data are the developments in non-linear inversion which have arisen in the context of the multi-frequency MT technique. The new approaches involve regularising an otherwise 'ill-posed' problem by introducing a smooth or minimum-structure constraint. In 2-D inversion, the problem of equivalence becomes particularly acute because of the larger number of degrees of freedom within the model space. The essential point is that the minimum-structure inversion concept acknowledges this fact and allows the construction of credible (non-extreme) resistivity models.

For 2-D MT inversion, deGroot-Hedlin and Constable (1990) implemented a minimum-structure inversion which is referred to as OCCAM and is based on the finite-element forward solution of Wannamaker et al. (1987). A more rapid 2D inversion code involving a non-linear, conjugate gradient (NLCG) algorithm has recently been described by Rodi and Mackie (1998). The algorithm implements first-derivative smoothing and includes a regularisation parameter ( $\tau$ ) that controls the degree of model smoothness/roughness (often a trade-off with misfit). VLF studies using the former method were described by Beamish (1994). The latter method is used in the present study since it readily permits the use of a regular subsurface finite-difference grid comprising in excess of 100x100 1 m cells. A limitation of the present algorithm is that joint inversion of VLF-R and VLF-Z data is not yet installed.

The measured data should possess error bounds. An *exact* fit between measured and modelled data is rarely warranted. The error bound must comprise the variance associated with physical measurement but it can also encompass the degree to which a particular level of modelling (e.g. 1D, 2D or 3D) is thought to be appropriate. Given a set of N observations ( $o_i$ ,  $i=1,N$ ) with standard errors ( $\sigma_i$ ), the concept is to only fit the observations to within a prescribed level of misfit. When the data and errors conform to Gaussian behaviour the chi-square ( $\chi^2$ ) statistic is a natural measure of misfit :

$$\chi^2 = \sum (o_i - m_i)^2 / \sigma_i^2$$

where  $m_i$  refers to the  $i$ 'th model response. An r.m.s. measure of misfit defined as  $\chi^2/N$  with an expectation value of unity is used here.

## 5.2) Application to field data

In order to implement the data inversion, it is assumed that the survey data, collected with the E-field in an E-W direction, conform to a TE-mode response. This is a realistic assumption in view of the related behaviour of both VLF-R and VLF-Z data (a pure TM-mode response does not produce a VLF-Z response). The assessment of structure along the Xylophagou profile is in terms of E-W striking resistivity variations.

A subsurface model grid comprising 201 10 m elements in the horizontal direction and 20 1 m elements in the vertical direction was developed. Beyond this central section, the grid expands to meet uniform boundary condition requirements. Below a depth of 20 m, the grid elements increase to 2, 3, 5 and 10 m thicknesses. The inversion was initiated using a half-space value of 250 ohm.m. A smoothing parameter of 3 was employed (Rodi and Mackie, 1998). Nominal data error assignments of 10% were applied to both apparent resistivity and phase data.

Inversion of the data resulted in an rms misfit of 1.5% (under the assumption of 10%) error bounds. A comparison of observed and modelled data is shown in Figure 5.1. It can be seen that all the main observed variations are adequately modelled. The resistivity model along the 2 km profile is shown in Figure 5.2 at a vertical exaggeration of x20. The colour-bar scale of resistivities is arranged to show high resistivities (100 to 1000 ohm.m and > 1000 ohm.m) which are taken to represent regions of highly intact limestone. Moderate resistivities (10 to 100 ohm.m) appear to represent the main 'background' resistivity along the profile. Several regions of very low resistivities are imaged. The main low resistivity region with an undulating upper surface (10 to 20 m deep) is located between 1400 and 1800 m. It is assumed that the low resistivity zones arise due to an increase in fracture intensity.

The resistivity distribution shown in Figure 5.2 is highly vertically exaggerated. The lateral configuration of the resistivity distribution is likely to be well resolved. The vertical extent of the zones is probably less well resolved. Due to the wide range of resistivities encountered, the maximum depth of the model shown in Figure 5.2 is unrealistic across the whole length of the profile.

In order to show the resistivity distribution at a more realistic scale, a portion of the model between 1400 and 1600 m, where the low resistivity zone is present, is shown at a vertical exaggeration of x2 in Figure 5.3. Along this section of the profile, resistivities in excess of 100 ohm.m are only associated with a small portion of the near-surface.

## 6) Summary

A 2 km profile of VLF data was acquired along a main N-S geophysical line crossing the Cape Pyla reef limestone. Both VLF-R and VLF-Z data were acquired. Attempts were made to obtain data from both N-S and E-W VLF transmissions. Due to poor signal strengths from N-S transmitters, only the E-W (E-field) transmissions of the HWE transmitter at a frequency of 18.3 kHz proved reliable.

Both VLF-R and VLF-Z 18.3 kHz data were acquired at 5 m intervals, with an E-W E-field, along the main profile from 100 to 2100 m. High wavenumber noise at the measurement scale is

apparent in both the VLF-R and VLF-Z data. Such noise is likely to be geological in origin and may be introduced by small-scale irregularities associated with near-surface features in the partially-exposed limestone crust (Kafkalla). In order to provide a regionally representative data set the raw data have been low-pass filtered.

The VLF-R data indicate a wide range of resistivities from 10 to over 1000 ohm.m. Both the VLF-R and VLF-Z data indicate a high degree of lateral resistivity variation across the profile. The joint behaviour of the VLF-R and VLF-Z data indicate that the response observed is a TE-mode responding primarily to E-W structural variations.

The VLF-R data, resampled at an interval of 10 m, have been inverted using a new NLCG algorithm. The response of the resulting resistivity model has an rms misfit of 1.6% when 10% observational errors are assumed. The resistivity model presented has regions of high resistivity (e.g. 100 to 1000 ohm.m and > 1000 ohm.m) both at shallow depths (< 10 m) and in vertical zones. These zones are tentatively taken to represent zones of highly intact limestone. Moderate resistivities (10 to 100 ohm.m) appear to represent the main 'background' resistivity along the profile. Several regions of very low resistivities (< 10 ohm.m) are imaged. The main low resistivity region with an undulating upper surface (10 to 20 m deep) is located between 1400 and 1800 m. It is assumed that the low resistivity zones arise due to an increase in fracture intensity.

## 7) References

- Beamish, D., 1994. Two-dimensional, regularised inversion of VLF data. *Journal of Applied Geophysics*, 32, 357-374.
- Beamish, D., 1998. Three-dimensional modelling of VLF data. *J. Applied Geophysics*, 39, 63-76.
- deGroot-Hedlin, C.M. and Constable, S.C., 1990. Occam's inversion to generate smooth, two-dimensional models from magnetotelluric data. *Geophysics*, 55: 1613-1624.
- Fischer, G., Le Quang, B.V. and Muller, I., 1983. VLF ground surveys, a powerful tool for the study of shallow two-dimensional structures. *Geophys. Prosp.*, 31: 977-991.
- McNeill, J.D. and Labson, V.F., 1991. Geological mapping using VLF radio fields. In: Nabighian, M. (Editor), *Electromagnetic Methods in Applied Geophysics, Part B: Application*. SEG, Tulsa, pp. 521-640.
- Rodi, W. and Mackie, R.L., 1998. Nonlinear conjugate gradients algorithm for 2-D magnetotelluric inversion, *Geophysics*, submitted.
- Strangway, D.W., Swift, Jr, C.M. and Holmer, R.C., 1973. The application of audio-frequency magnetotellurics (AMT) to mineral exploration. *Geophysics*, 38: 1159-1175.
- Tabbagh, A., Benderitter, Y., Andrieux, P., Decriaud, J.P. and Guerin, R., 1991. VLF resistivity mapping and verticalization of the electric field. *Geophys. Prosp.*, 39: 1083-1097.

Wannamaker, P.E., Stodt, J.A. and Rijo, L., 1987. A stable finite element solution for two-dimensional magnetotelluric modelling. *Geophys. J. R. astr. Soc.*, **88**: 277-296.

## **8) Acknowledgements**

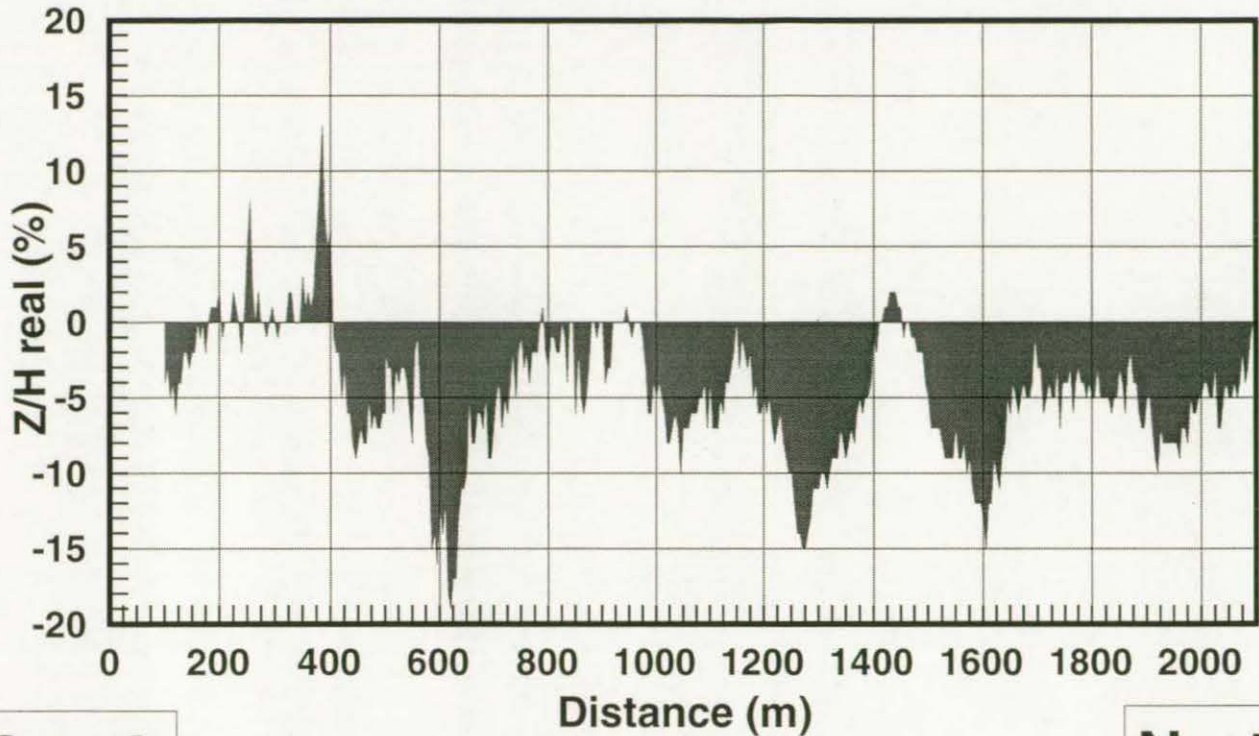
It is a pleasure to acknowledge the major contribution made by the GSD, Nicosia during the field work. Many members of staff were involved and I thank them all.



Fig. 4.1

**Xylophagu VLF survey 1998**

**18.3 kHz E-W 5m interval**



**South**

**North**

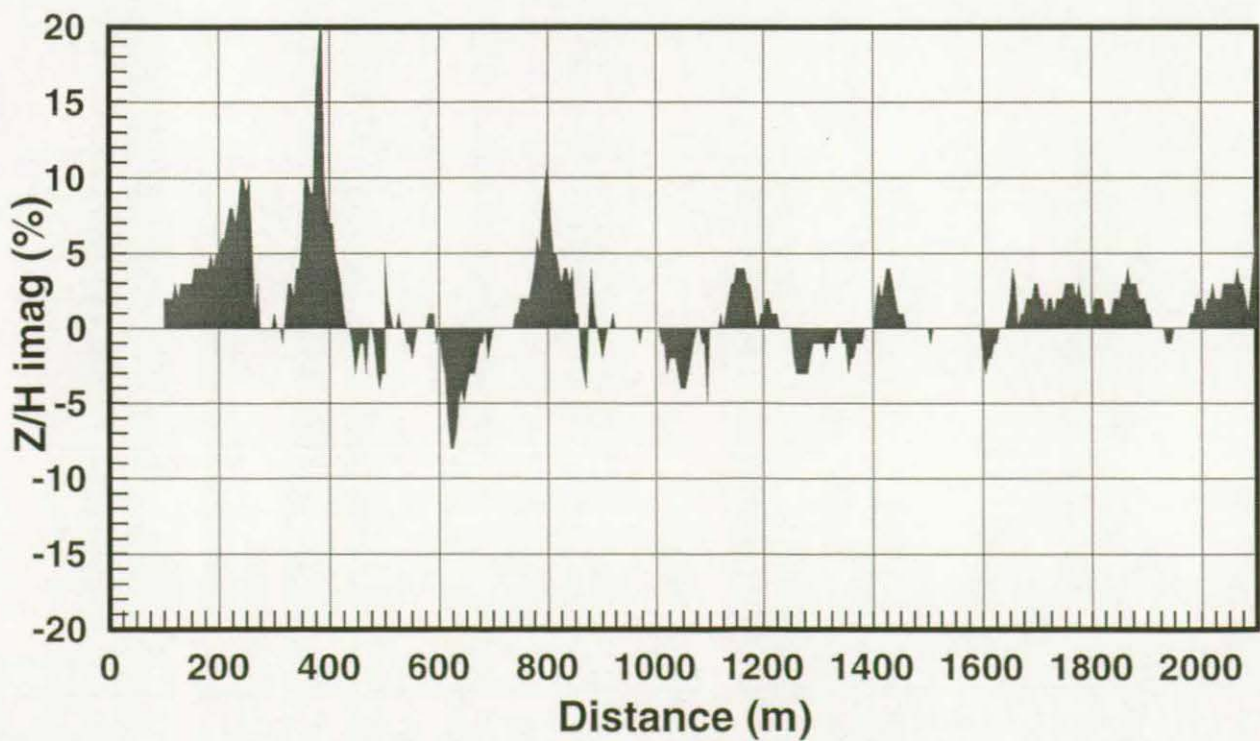


Fig. 4.2

**Xylophagu VLF survey 1998**

**18.3 kHz E-W 5m interval**

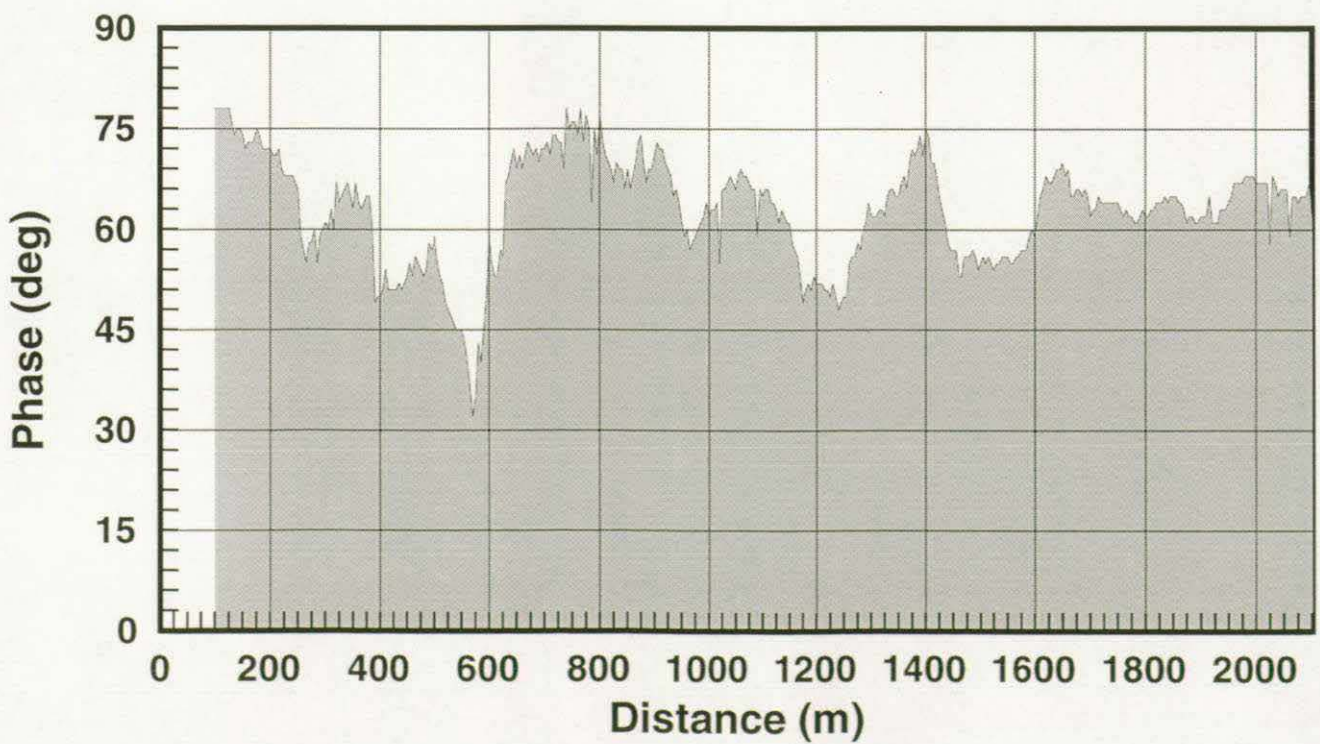
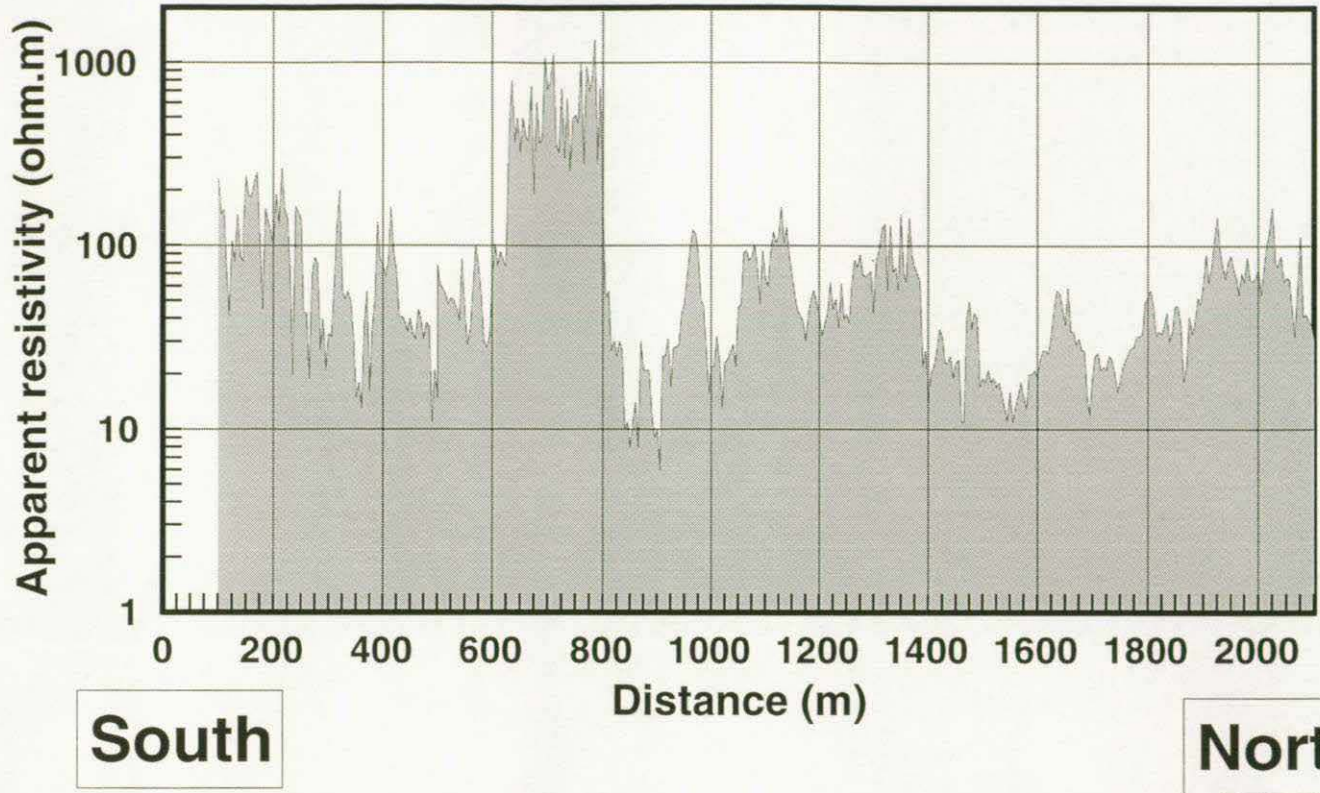


Fig. 4.3

**Xylophagu VLF survey 1998**

**18.3 kHz E-W 5m interval, 50 m LP**

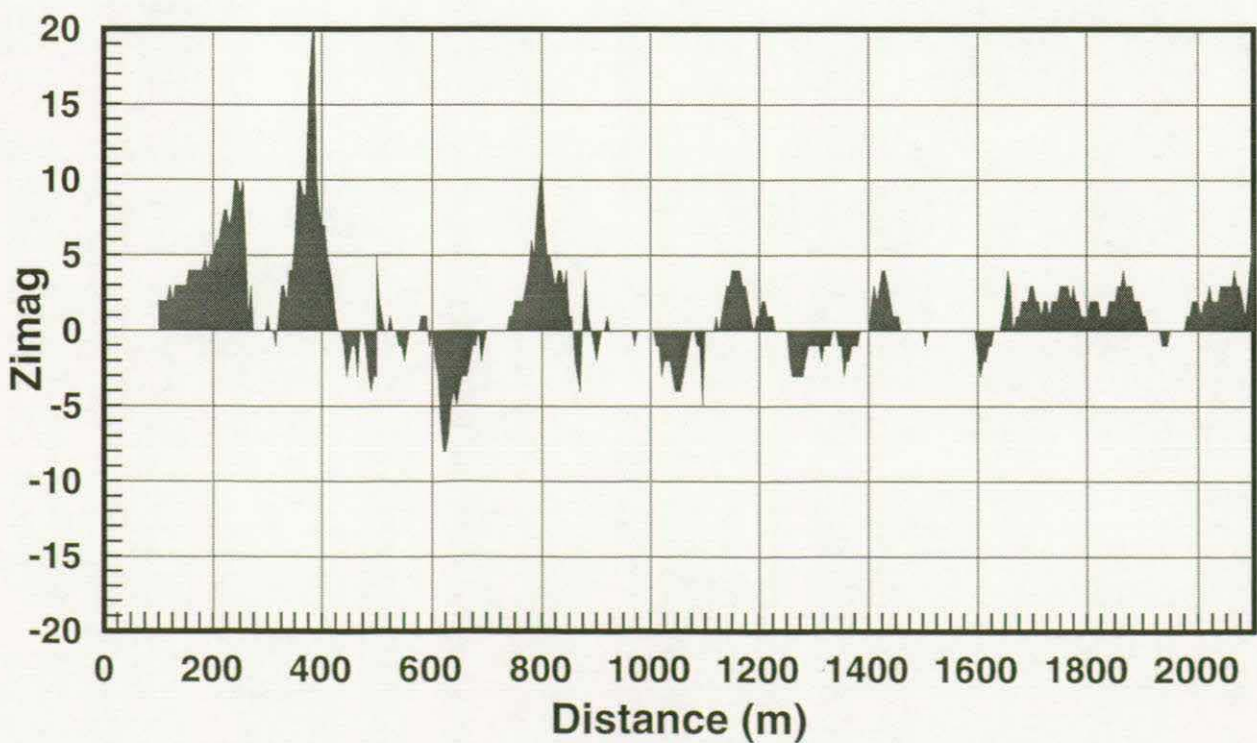
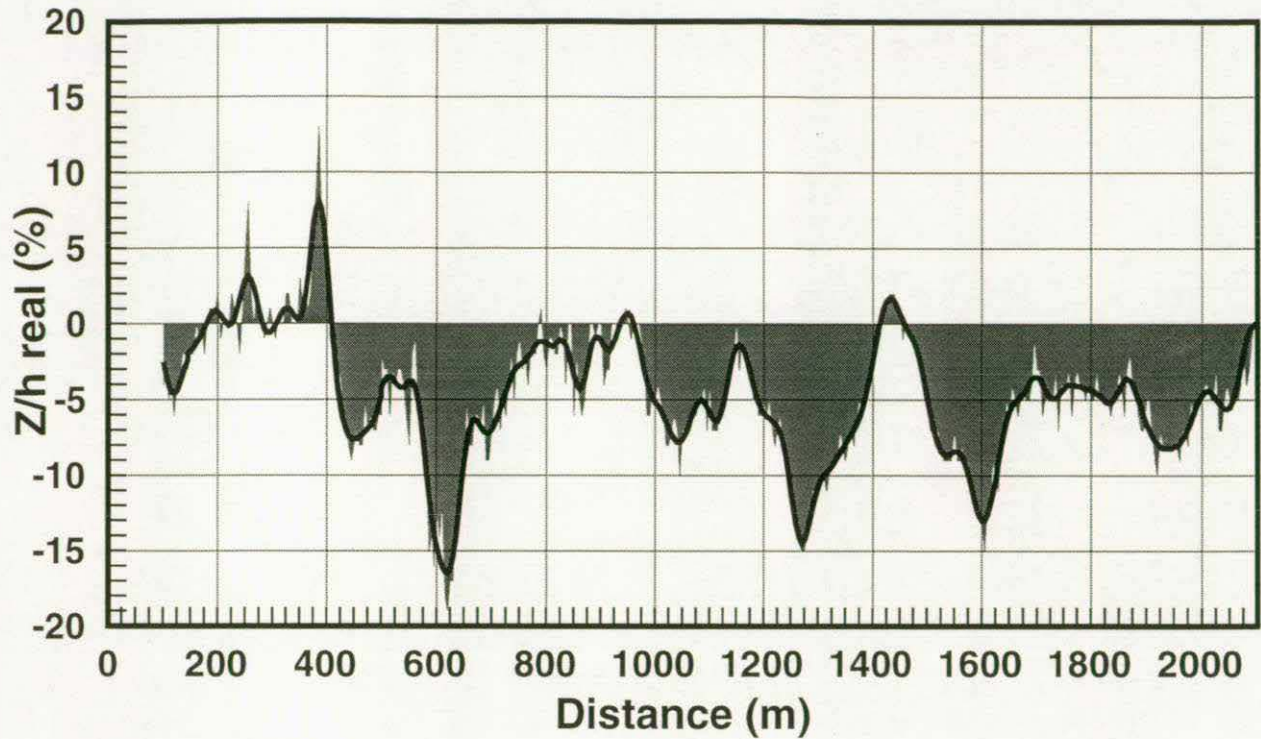
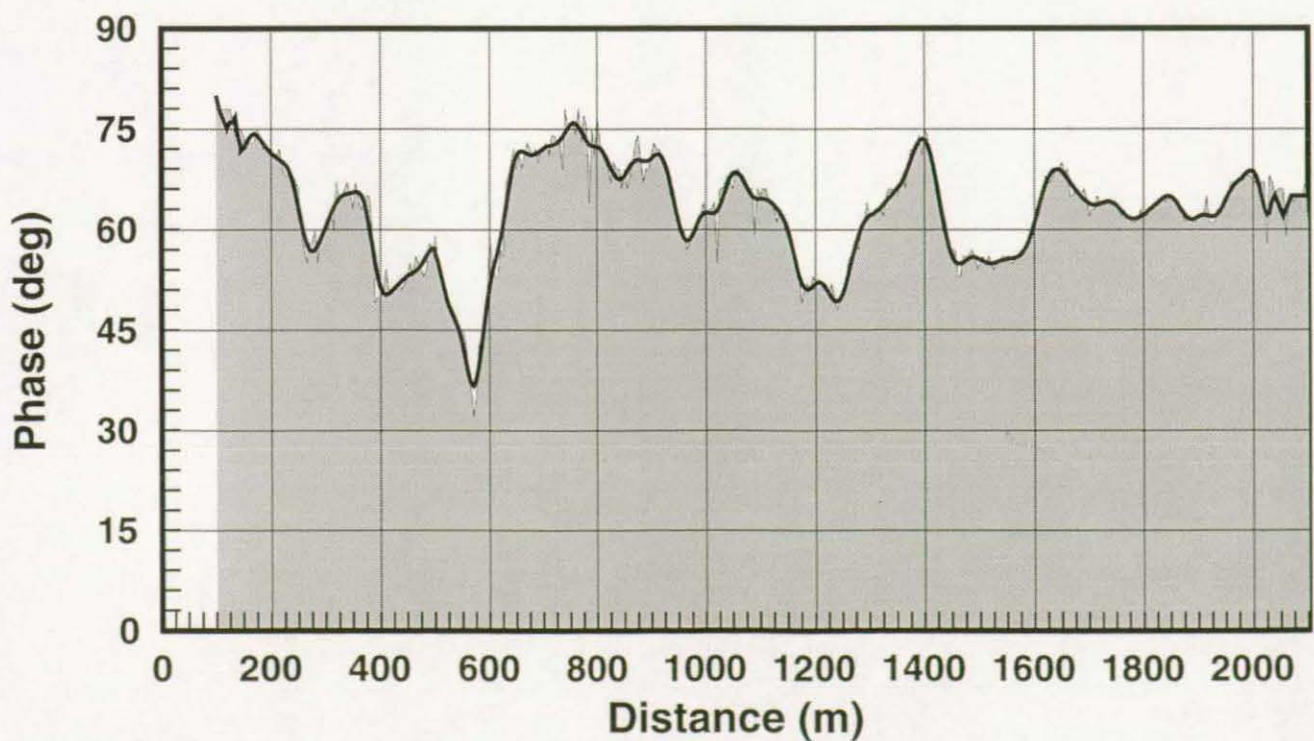
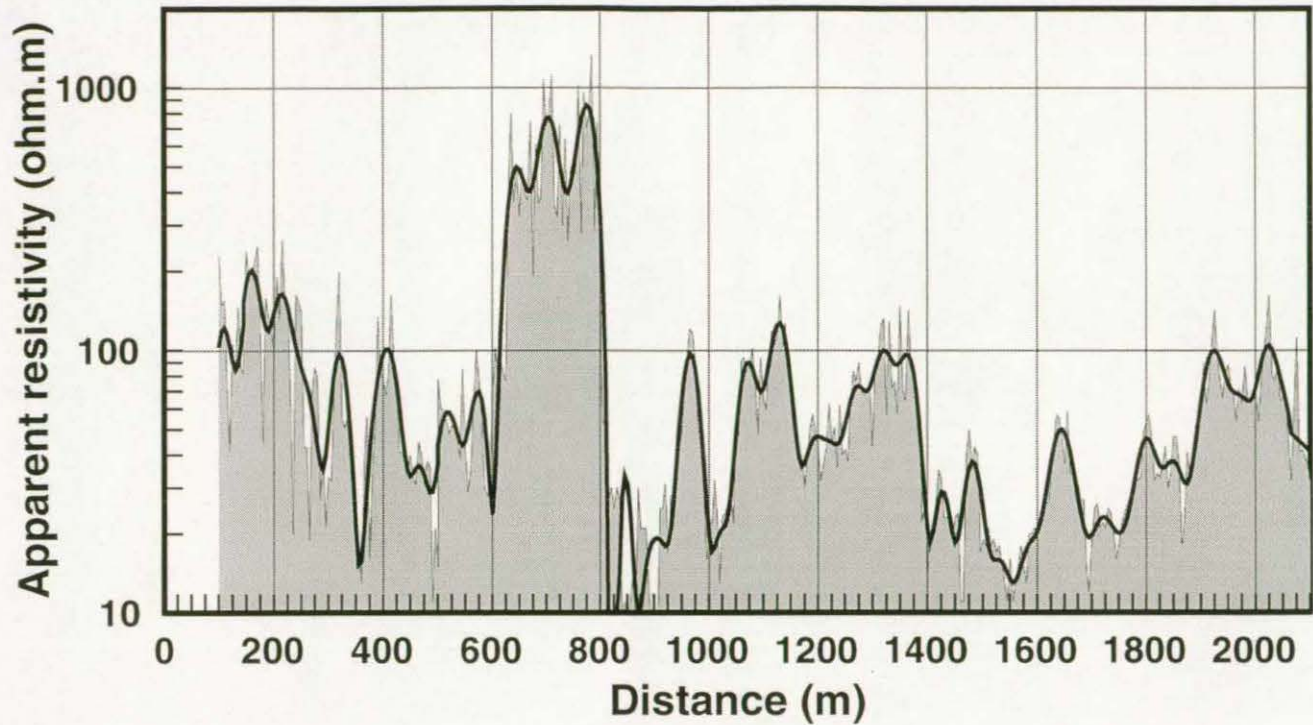


Fig. 4.4

**Xylophagu VLF survey 1998**

**18.3 kHz E-W 5m interval, 50 m LP**

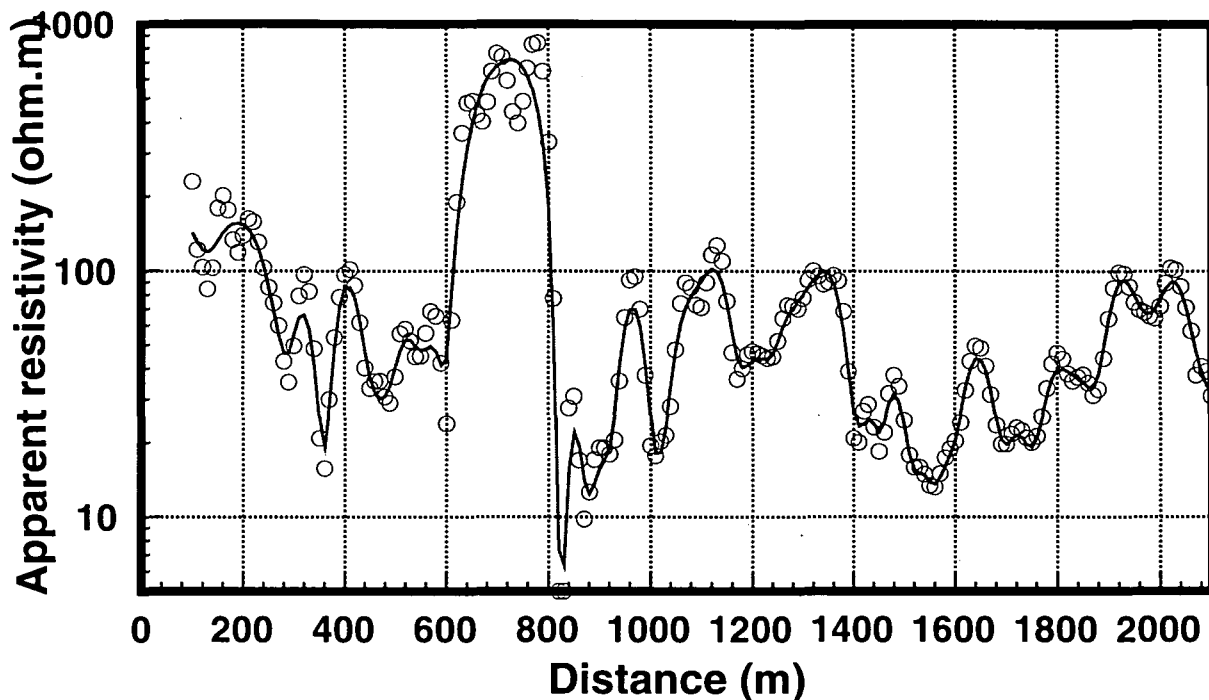


# Xylophagu VLF survey 1998

18.3 kHz E-W 10 m interval

Comparison of observed and modelled results

TE-mode. 2d NLCG. 10% data errors gives rms misfit of 1.5%



South

North

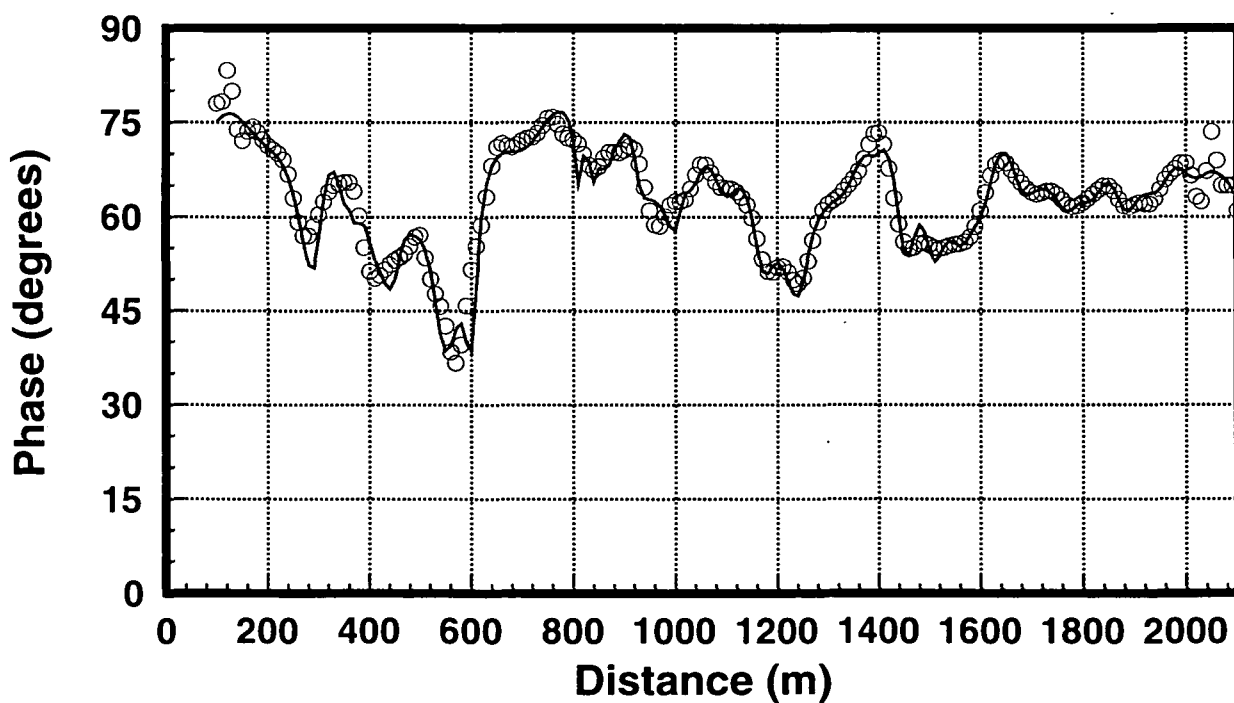
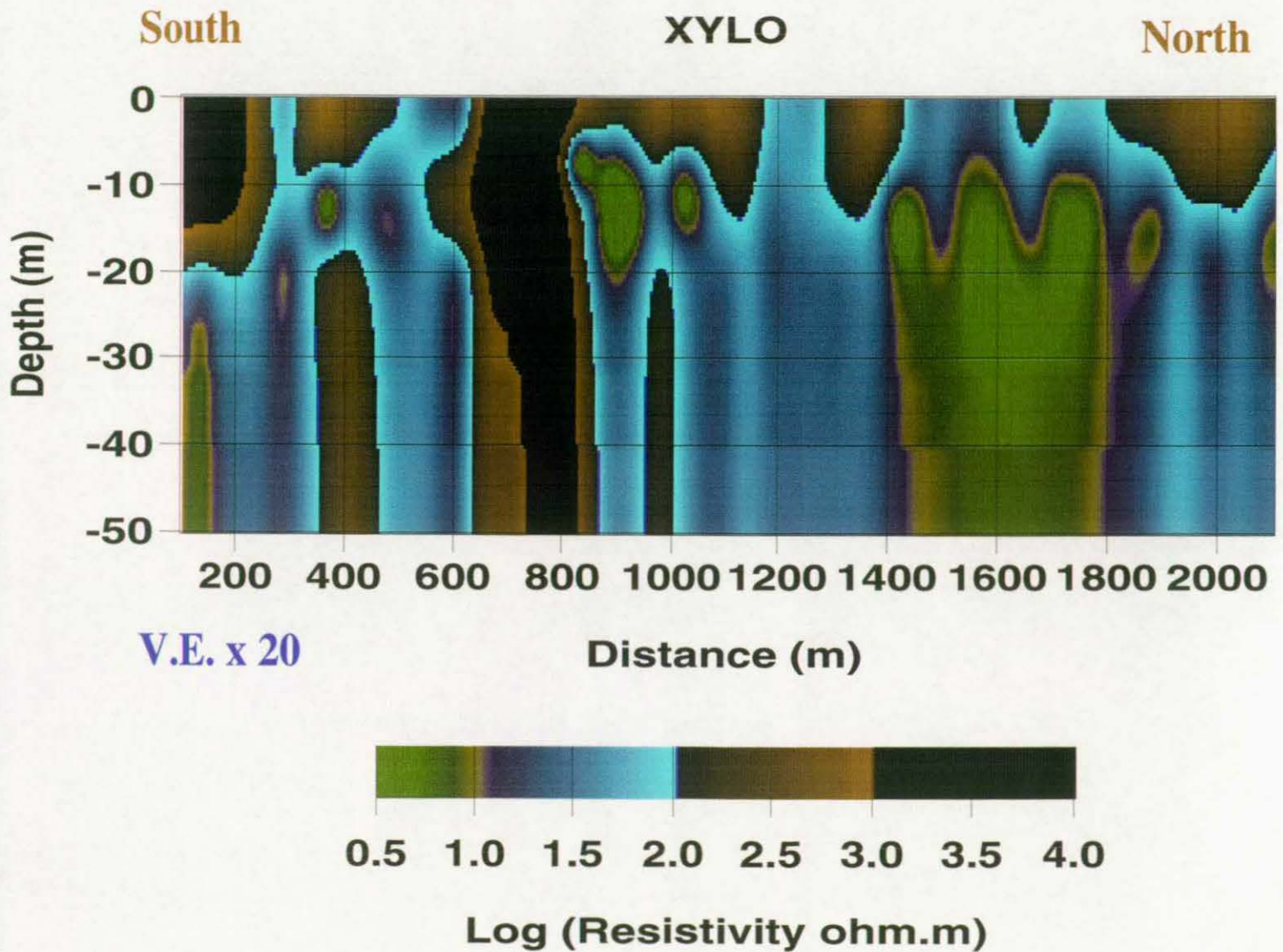


**Fig. 5.2**

**Cyprus VLF survey 98**

**Xylophagu 18.3 kHz TE**

**2D resistivity model using NLCG inversion**



TE-mode. 2d bNLCG. 10%data errors give misfit of 1.6%

Filtered data at 10 m, 201 observations of apparent resistivity and phase

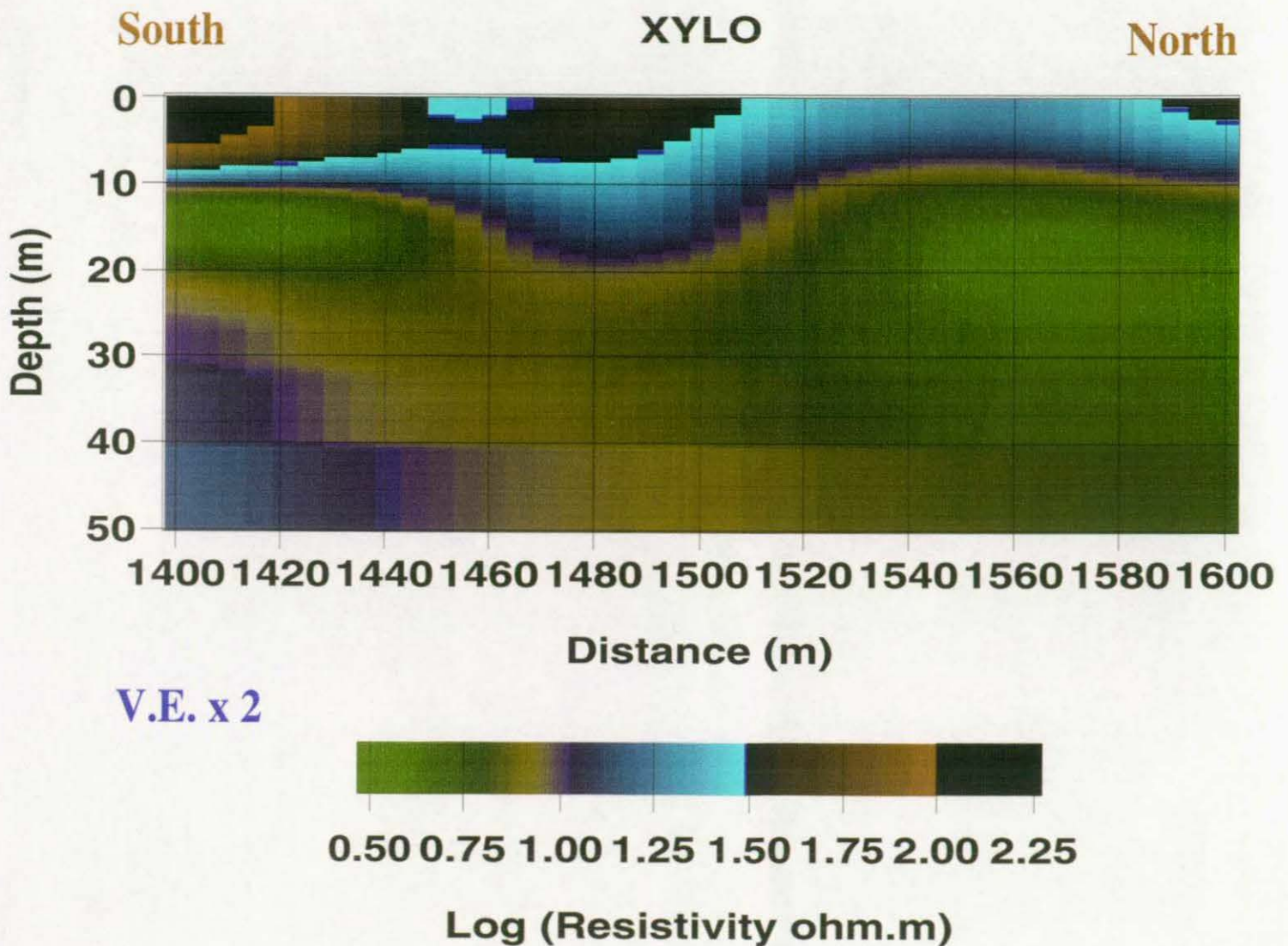
**Fig. 5.3**

**Cyprus VLF survey 98**

**Xylophagu 18.3 kHz TE**

**2D resistivity model using NLCG inversion**

**200 m detail from model**



TE-mode. 2d bNLCG. 10% data errors give misfit of 1.6%

Filtered data at 10 m, 201 observations of apparent resistivity and phase

BRITISH GEOLOGICAL SURVEY

Fluid Processes and Waste Management Group

TECHNICAL REPORT WE/98/49

**VLF surveys on Cyprus:  
Xylophagou, 1998**

David Beamish

*Bibliographic Reference :*  
Beamish D., 1998.  
*VLF Surveys on Cyprus:  
Xylophagou, 1998.*  
British Geological Survey,  
Technical Report, WE/98/49

A report prepared for:  
European Commission  
DG-XII  
Directorate B  
Programme INCO-DC  
75, Rue Montoyer  
B-1040 Brussels



British Geological Survey, Keyworth, Nottingham, 1998

©NERC copyright 1998



## CONTENTS

<b>1) Introduction</b>	<b>2</b>
<b>2) The VLF Technique</b>	<b>2</b>
<b>3) Cyprus Field Work</b>	<b>3</b>
<b>3.1 Xylophagou Field Area</b>	<b>3</b>
<b>3.2 VLF data acquisition</b>	<b>4</b>
<b>4) Data for the Xylophagou profile</b>	<b>4</b>
<b>5) 2D regularised inversion of VLF data</b>	<b>5</b>
<b>5.1 Theory</b>	<b>5</b>
<b>5.2) Application to field data</b>	<b>6</b>
<b>6) Summary</b>	<b>6</b>
<b>7) References</b>	<b>7</b>
<b>8) Acknowledgements</b>	<b>8</b>

---

## 1) Introduction

This report summarises the results of work undertaken for the EEC INCO-DC project: A new integrated geophysical approach for the rational management and exploration of groundwater resources. The programme Project Number is 950176 under Contract Number ERBIC 18 CT 960122.

EU member participants are:

The Netherlands:	RGD: (NITG-TNO), Haarlem James Baker (Project Coordinator)	
France:	BRGM, Orleans Alain Beauce	
U.K.:	BGS, Nottingham D. Beamish and Jon Busby	

Non-EU partners are:

Cyprus:	GSD, Nicosia Sortiris Kramvis	GEOINVEST, Nicosia Andreas Shiathas
Israel:	GII, Holon Mark Goldman	

This report summarises the field activities of the VLF (Very Low Frequency EM) technique which took place on Cyprus during May and June 1998. Geophysical surveys on Cyprus are designated as Task 3 and the VLF technique designated as sub-task 3.8. VLF fieldwork took place mainly along a main N-S profile in the Xylofagou area of eastern Cyprus. VLF observations along more limited traverses also took place at a few selected localities on the pillow lavas in the Troodos area. This report describes only the VLF survey in the Xylofagou area.

## 2) The VLF technique

The VLF survey technique is a well-established electromagnetic (EM) method of applied geophysics. McNeill and Labson (1991) review its use for geological and hydrogeological applications. The method is one of a class of EM techniques that conform to a plane-wave sounding of subsurface resistivity structure; a closely allied (natural-field) technique is the audiomagnetotelluric (AMT) method (e.g. Strangway et al., 1973). The VLF-EM technique makes use of one or more distant radio transmitters operating between 15 and 30 kHz. The limited bandwidth means that, although several measurements may be obtained at different frequencies (using different transmitters), a main attribute of the method is that of a single frequency sounding. The fact that the instrumentation is very portable and cost-effective survey method compensate for the lack of bandwidth. The VLF method was developed as an inductive

sounding technique measuring the amplitude and (subsequently) phase relationship between the vertical (secondary) magnetic field (Z) relative to the horizontal primary field (H). This method, referred to here as VLF-Z, relies on wavefield interaction with two-dimensional (2-D) and three-dimensional (3-D) resistivity structure. The technique has since been extended to include a measure of the induced horizontal electric field (E) component. This VLF-R measurement provides an impedance value (e.g. E/H), usually expressed as apparent resistivity and phase, using short (e.g. 5 m) electric dipoles. The VLF-R measurement, although appropriate for a one-dimensional (1-D) application, contains only marginal information on the vertical resistivity structure (Fischer et al., 1983) because, in effect, only a single frequency is available. These factors suggest that the strength of VLF methods lie predominantly in the definition of lateral gradients in the subsurface resistivity structure. The interpretation problem is therefore, at least, two-dimensional.

As discussed by Fischer et al. (1983) and Beamish (1998), in order to ensure consistency with a 2-D approach, the directional VLF data must conform to one of the two principal modes of 2-D induction. The assumption of infinite strike (which defines the 2-D case) provides two decoupled modes involving separate combinations of the field components. The TE-mode (or E-polarisation, electric field parallel to strike) involves surface fields of  $E_x$ ,  $H_y$  and  $H_z$ . The TM-mode (or H-polarisation, magnetic field parallel to strike) involves the surface fields  $H_x$ ,  $E_y$  and  $E_z$ .

Due to the directional nature of VLF measurements, we require therefore that the measurements be made in, at least one, of the two principal directions. Where the geological strike is not known, the sensible survey option of taking measurements from several azimuthally distinct transmitters may be used.

### 3) Cyprus Field Work

#### 3.1 Xylophagou Field Area

The hydrogeology of the field area is described in an unpublished report prepared for the fieldwork by Geoinvest Ltd. The report describes the main Kokkinokhoria aquifer as the major and most productive part of the general SE Mesaoria aquifer and provides details of its overexploitation. A secondary limestone crust (Kafkalla) and deep red soils tend to obscure the surface features of the area. Four main aquiferous units are recognised: (a) the sandy aquifer, made up of the upper sandy section of a Plio-Pleistocene sequence extending throughout the SE Mesaoria, (b) the limestone aquifer of the Miocene reef limestone facies which is in contact with the sandy aquifer, (c) the gypsum aquifer at the top of the Middle Miocene sequence containing highly saline water and (d) the chalk aquifer of the Palaeocene – Lower Miocene sequence.

The aquifer tends to be compartmentalised in a series of vertical faults. A normal E-W fault, south of Xylophagou, separates the Cape Pyla horst, mainly of reef limestone, from the aquifer. Figure 3.1 shows the field area and an initial location map of the main N-S geophysical traverse. The profile origin is located in the south and the traverse crosses the main reef limestone. Boreholes GR33 (to the west of the profile), 30/40 (close to the profile) and 92/52 (to the east of the profile) can be used as control. The borehole log of GR33 has a depth of 222.5 m and indicates chalk and marly chalk to a depth of 15 m, below this depth the log records a crystalline

porous and cavernous dolomitic and reef limestone. Borehole 30/40 is 300 m east of the traverse (1600 m along the line) and the log records 44.2 m of limestone. The borehole log of 92/52 records 21 m of hard white limestone.

### 3.2 VLF data acquisition

VLF data collection took place between May 30 and June 08 1998. The measurements were made with the Scintrex IGS-2 equipment, using 5 metre, capacitively-coupled E-field dipoles. The equipment has a reading resolution of 1% in the case of the VLF-Z components and 1 ohm.m and 1 degree in the case of the VLF-R measurements.

A systematic study of VLF horizontal magnetic field signal strengths was conducted across the bandwidth from 15 to 30 kHz. In contrast to Western Europe, all transmissions on Cyprus were found to be weak and often close-to or below the noise level of the instrument. Transmissions providing a N-S E-field were a particular problem. The strongest N-S transmissions were found at frequencies of 18.0, 18.1 and 23.5 kHz. In practice, all the N-S signals were found to be intermittent. The most reliable and strong VLF transmission providing an E-W E-field was the 18.3 kHz transmission (HWE, Le Blanc, France). This frequency was used extensively during the survey.

Skin-depths at 18.3 kHz range from 11.8 m (in 10 ohm.m material), to 26.3 m (in 50 ohm.m material) through to 37.2 m (in 100 ohm.m) material. VLF penetration depths, in uniform materials, are a factor of 1.5 greater than the skin-depth.

## 4) Data for the Xylofagou profile

VLF data were collected at 5 m intervals along the main N-S geophysical traverse that ran from near the coast (i.e. towards the profile origin) in the south and northwards (inland). VLF data were collected along the profile from 100 m through to 2100 m. The data were collected over several days. In each case attempts were made to collect VLF-R and VLF-Z using two orthogonal (N-S and E-W) transmitters. The only reliable transmissions were those at 18.3 KHz, which were measured using E-W electric field dipoles. As a consequence the only continuous (i.e. every 5 m) data set was obtained using the E-W 18.3 kHz signal.

The complete VLF-Z set for the Xylophagu profile is shown in Figure 4.1 from 100 to 2100 m. Despite the fact that high-wavenumber noise is apparent at the data sampling interval, significant longer wavelength features can be observed in both real and imaginary components. There appears to be a transition at 400-500 m along the profile. In general, the real response is largely negative while the imaginary response is only slightly positive.

The corresponding VLF-R data set along the profile is shown in Figure 4.2. A logarithmic scale for apparent resistivity has been used due to the large range of values encountered (from < 10 to > 1000 ohm.m). In broad terms, the majority of apparent resistivity values lie in the range 10 to 100 ohm.m while the phase values are generally > 45 degrees. Again, despite the fact that high-wavenumber noise is apparent at the data sampling interval, significant longer wavelength features can be observed in both amplitude and phase values.

In order to extract reliable information at a regional scale across the profile, the raw data shown in Figures 4.1 and 4.2 have been low-pass filtered. A finite-impulse response filter with a low cut point at 50 m was designed and applied to the two data sets. The raw and low-pass filtered data are shown in Figures 4.3 (VLF-Z) and 4.4 (VLF-R).

The filtered data set comprises 201 data points resampled every 10 m, between 100 and 2100 m. These data have been used to investigate the resistivity distribution along the traverse.

## 5) 2D regularised inversion of VLF data

### 5.1 Theory

The starting point in the modelling of VLF data are the developments in non-linear inversion which have arisen in the context of the multi-frequency MT technique. The new approaches involve regularising an otherwise 'ill-posed' problem by introducing a smooth or minimum-structure constraint. In 2-D inversion, the problem of equivalence becomes particularly acute because of the larger number of degrees of freedom within the model space. The essential point is that the minimum-structure inversion concept acknowledges this fact and allows the construction of credible (non-extreme) resistivity models.

For 2-D MT inversion, deGroot-Hedlin and Constable (1990) implemented a minimum-structure inversion which is referred to as OCCAM and is based on the finite-element forward solution of Wannamaker et al. (1987). A more rapid 2D inversion code involving a non-linear, conjugate gradient (NLGG) algorithm has recently been described by Rodi and Mackie (1998). The algorithm implements first-derivative smoothing and includes a regularisation parameter ( $\tau$ ) that controls the degree of model smoothness/roughness (often a trade-off with misfit). VLF studies using the former method were described by Beamish (1994). The latter method is used in the present study since it readily permits the use of a regular subsurface finite-difference grid comprising in excess of 100x100 1 m cells. A limitation of the present algorithm is that joint inversion of VLF-R and VLF-Z data is not yet installed.

The measured data should possess error bounds. An *exact* fit between measured and modelled data is rarely warranted. The error bound must comprise the variance associated with physical measurement but it can also encompass the degree to which a particular level of modelling (e.g. 1D, 2D or 3D) is thought to be appropriate. Given a set of N observations ( $o_i$ ,  $i=1,N$ ) with standard errors ( $\sigma_i$ ), the concept is to only fit the observations to within a prescribed level of misfit. When the data and errors conform to Gaussian behaviour the chi-square ( $\chi^2$ ) statistic is a natural measure of misfit :

$$\chi^2 = \sum (o_i - m_i)^2 / \sigma_i^2$$

where  $m_i$  refers to the  $i$ 'th model response. An r.m.s. measure of misfit defined as  $\chi^2/N$  with an expectation value of unity is used here.

## 5.2) Application to field data

In order to implement the data inversion, it is assumed that the survey data, collected with the E-field in an E-W direction, conform to a TE-mode response. This is a realistic assumption in view of the related behaviour of both VLF-R and VLF-Z data (a pure TM-mode response does not produce a VLF-Z response). The assessment of structure along the Xylophagou profile is in terms of E-W striking resistivity variations.

A subsurface model grid comprising 201 10 m elements in the horizontal direction and 20 1 m elements in the vertical direction was developed. Beyond this central section, the grid expands to meet uniform boundary condition requirements. Below a depth of 20 m, the grid elements increase to 2, 3, 5 and 10 m thicknesses. The inversion was initiated using a half-space value of 250 ohm.m. A smoothing parameter of 3 was employed (Rodi and Mackie, 1998). Nominal data error assignments of 10% were applied to both apparent resistivity and phase data.

Inversion of the data resulted in an rms misfit of 1.5% (under the assumption of 10%) error bounds. A comparison of observed and modelled data is shown in Figure 5.1. It can be seen that all the main observed variations are adequately modelled. The resistivity model along the 2 km profile is shown in Figure 5.2 at a vertical exaggeration of x20. The colour-bar scale of resistivities is arranged to show high resistivities (100 to 1000 ohm.m and > 1000 ohm.m) which are taken to represent regions of highly intact limestone. Moderate resistivities (10 to 100 ohm.m) appear to represent the main 'background' resistivity along the profile. Several regions of very low resistivities are imaged. The main low resistivity region with an undulating upper surface (10 to 20 m deep) is located between 1400 and 1800 m. It is assumed that the low resistivity zones arise due to an increase in fracture intensity.

The resistivity distribution shown in Figure 5.2 is highly vertically exaggerated. The lateral configuration of the resistivity distribution is likely to be well resolved. The vertical extent of the zones is probably less well resolved. Due to the wide range of resistivities encountered, the maximum depth of the model shown in Figure 5.2 is unrealistic across the whole length of the profile.

In order to show the resistivity distribution at a more realistic scale, a portion of the model between 1400 and 1600 m, where the low resistivity zone is present, is shown at a vertical exaggeration of x2 in Figure 5.3. Along this section of the profile, resistivities in excess of 100 ohm.m are only associated with a small portion of the near-surface.

## 6) Summary

A 2 km profile of VLF data was acquired along a main N-S geophysical line crossing the Cape Pyla reef limestone. Both VLF-R and VLF-Z data were acquired. Attempts were made to obtain data from both N-S and E-W VLF transmissions. Due to poor signal strengths from N-S transmitters, only the E-W (E-field) transmissions of the HWE transmitter at a frequency of 18.3 kHz proved reliable.

Both VLF-R and VLF-Z 18.3 kHz data were acquired at 5 m intervals, with an E-W E-field, along the main profile from 100 to 2100 m. High wavenumber noise at the measurement scale is

apparent in both the VLF-R and VLF-Z data. Such noise is likely to be geological in origin and may be introduced by small-scale irregularities associated with near-surface features in the partially-exposed limestone crust (Kafkalla). In order to provide a regionally representative data set the raw data have been low-pass filtered.

The VLF-R data indicate a wide range of resistivities from 10 to over 1000 ohm.m. Both the VLF-R and VLF-Z data indicate a high degree of lateral resistivity variation across the profile. The joint behaviour of the VLF-R and VLF-Z data indicate that the response observed is a TE-mode responding primarily to E-W structural variations.

The VLF-R data, resampled at an interval of 10 m, have been inverted using a new NLCCG algorithm. The response of the resulting resistivity model has an rms misfit of 1.6% when 10% observational errors are assumed. The resistivity model presented has regions of high resistivity (e.g. 100 to 1000 ohm.m and > 1000 ohm.m) both at shallow depths (< 10 m) and in vertical zones. These zones are tentatively taken to represent zones of highly intact limestone. Moderate resistivities (10 to 100 ohm.m) appear to represent the main 'background' resistivity along the profile. Several regions of very low resistivities (< 10 ohm.m) are imaged. The main low resistivity region with an undulating upper surface (10 to 20 m deep) is located between 1400 and 1800 m. It is assumed that the low resistivity zones arise due to an increase in fracture intensity.

## 7) References

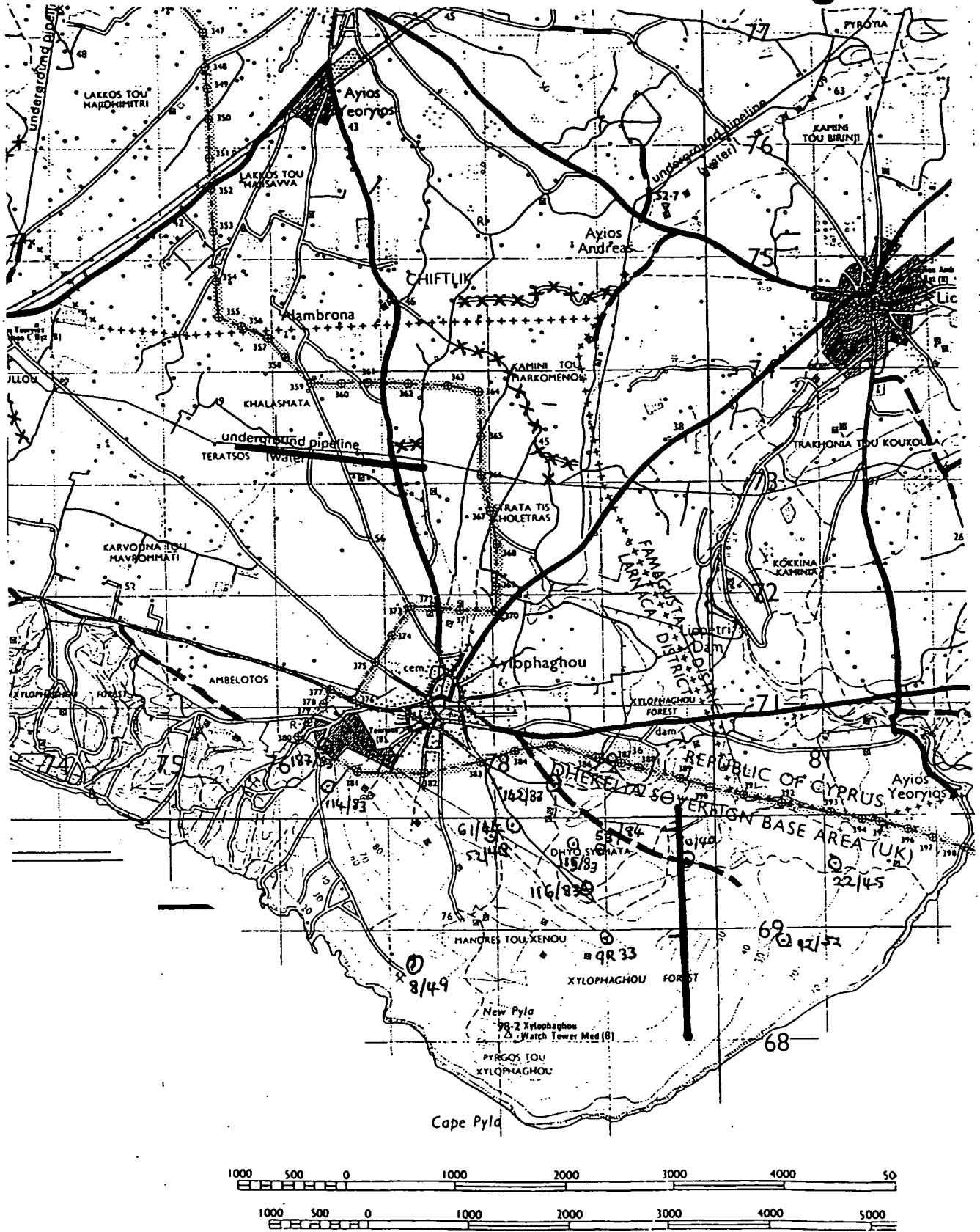
- Beamish, D., 1994. Two-dimensional, regularised inversion of VLF data. *Journal of Applied Geophysics*, 32, 357-374.
- Beamish, D., 1998. Three-dimensional modelling of VLF data. *J. Applied Geophysics*, 39, 63-76.
- deGroot-Hedlin, C.M. and Constable, S.C., 1990. Occam's inversion to generate smooth, two-dimensional models from magnetotelluric data. *Geophysics*, 55: 1613-1624.
- Fischer, G., Le Quang, B.V. and Muller, I., 1983. VLF ground surveys, a powerful tool for the study of shallow two-dimensional structures. *Geophys. Prosp.*, 31: 977-991.
- McNeill, J.D. and Labson, V.F., 1991. Geological mapping using VLF radio fields. In: Nabighian, M. (Editor), *Electromagnetic Methods in Applied Geophysics, Part B: Application*. SEG, Tulsa, pp. 521-640.
- Rodi, W. and Mackie, R.L., 1998. Nonlinear conjugate gradients algorithm for 2-D magnetotelluric inversion, *Geophysics*, submitted.
- Strangway, D.W., Swift, Jr, C.M. and Holmer, R.C., 1973. The application of audio-frequency magnetotellurics (AMT) to mineral exploration. *Geophysics*, 38: 1159-1175.
- Tabbagh, A., Benderitter, Y., Andrieux, P., Decriaud, J.P. and Guerin, R., 1991. VLF resistivity mapping and verticalization of the electric field. *Geophys. Prosp.*, 39: 1083-1097.

Wannamaker, P.E., Stodt, J.A. and Rijo, L., 1987. A stable finite element solution for two-dimensional magnetotelluric modelling. *Geophys. J. R. astr. Soc.*, **88**: 277-296.

## **8) Acknowledgements**

It is a pleasure to acknowledge the major contribution made by the GSD, Nicosia during the field work. Many members of staff were involved and I thank them all.

Fig. 3.1

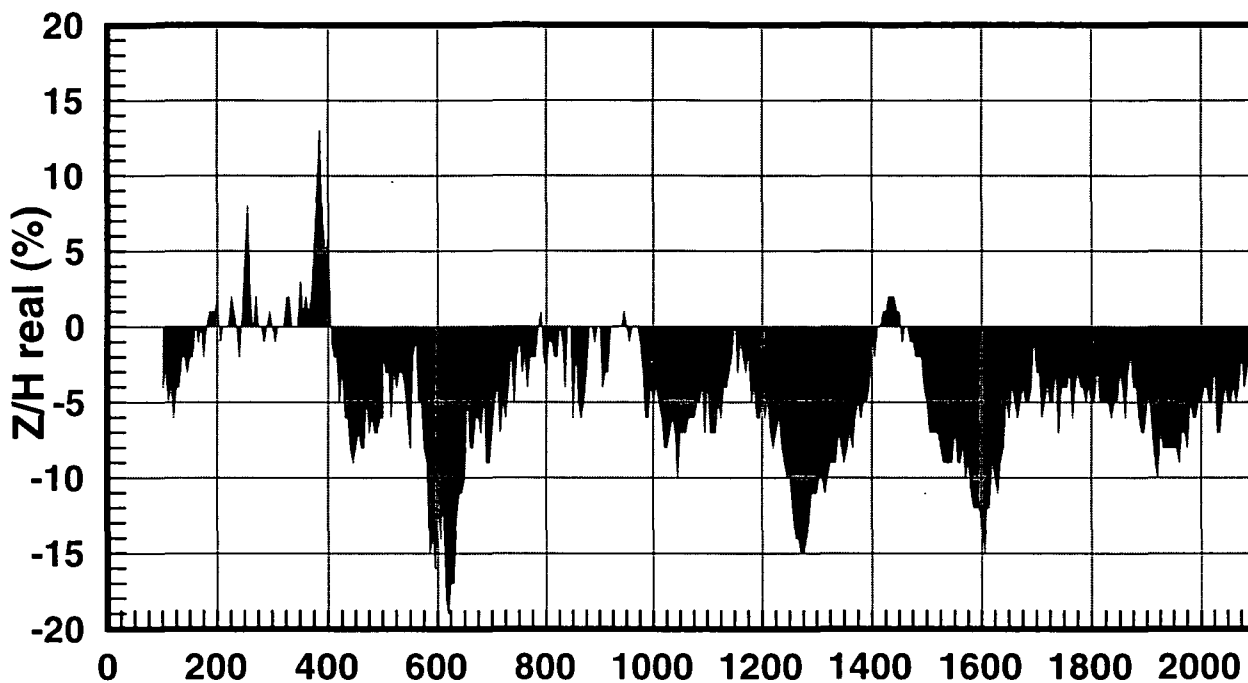


**Xylophagou VLF survey location (provisional)**

Fig. 4.1

**Xylophagu VLF survey 1998**

**18.3 kHz E-W 5m interval**



**South**

**North**

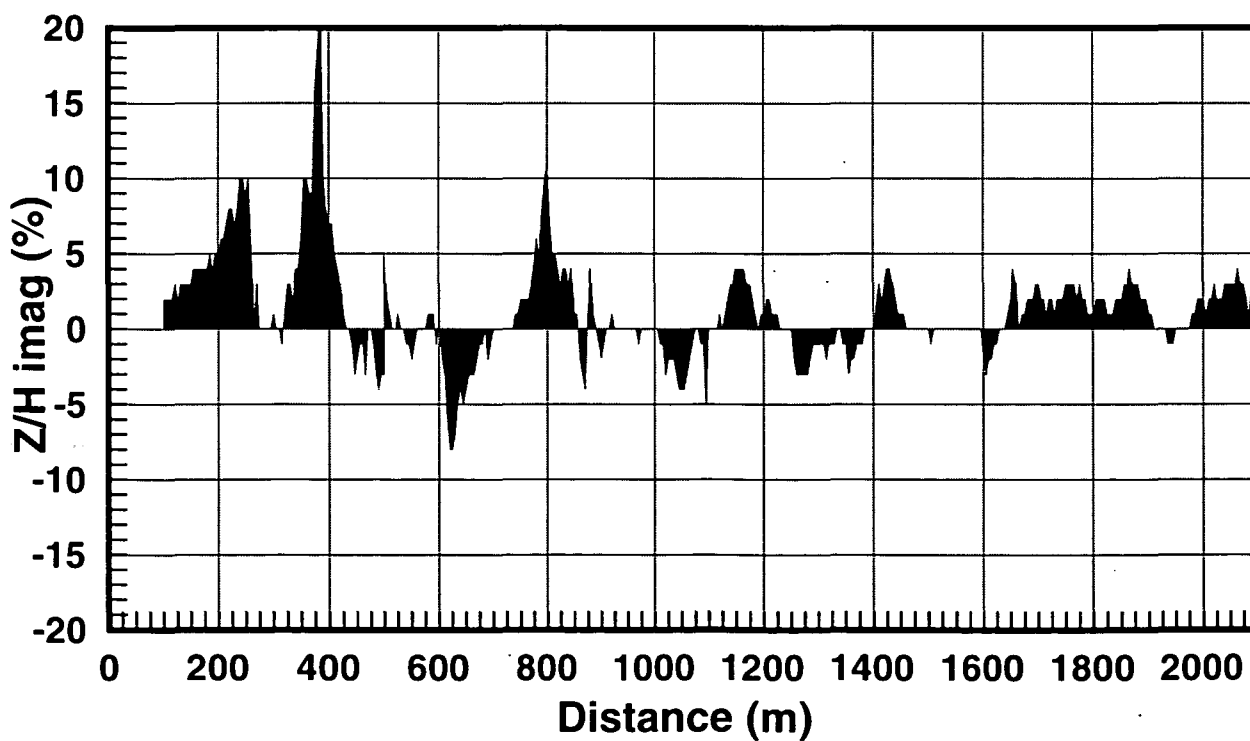
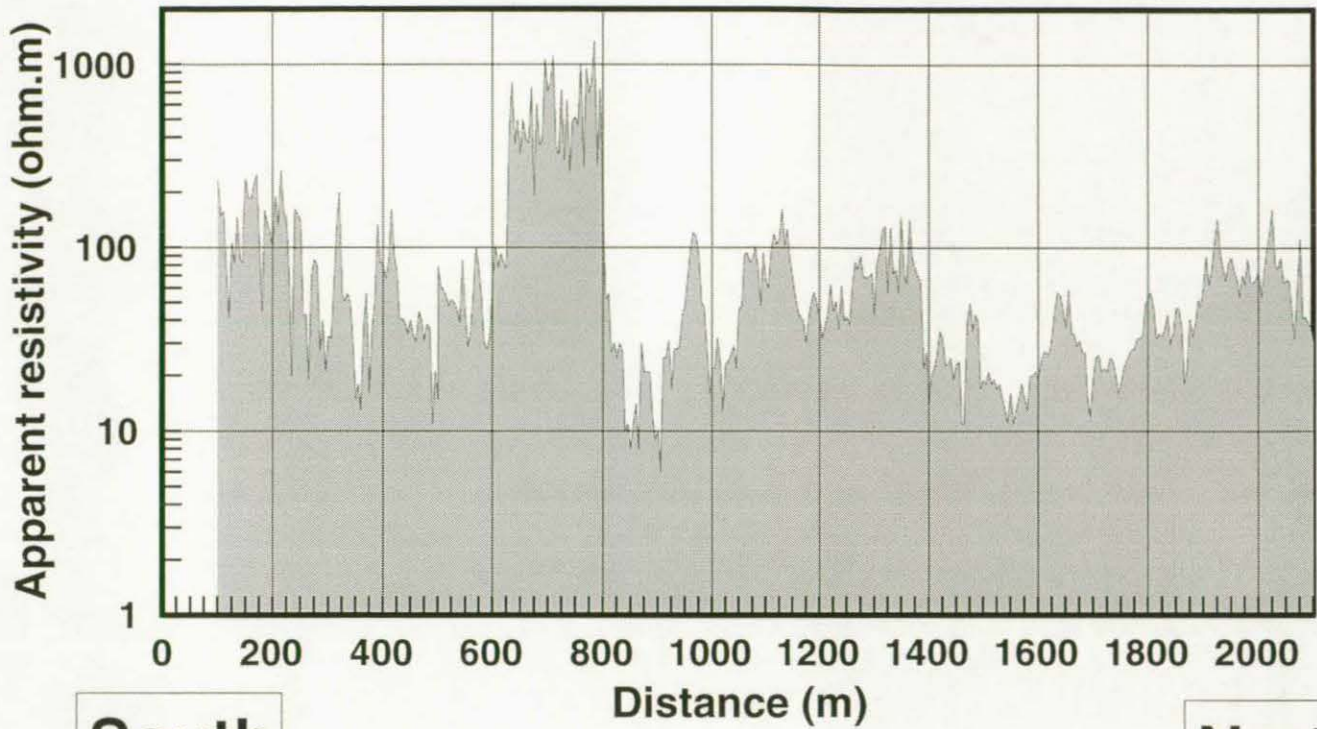


Fig. 4.2

**Xylophagu VLF survey 1998**

**18.3 kHz E-W 5m interval**



**South**

**North**

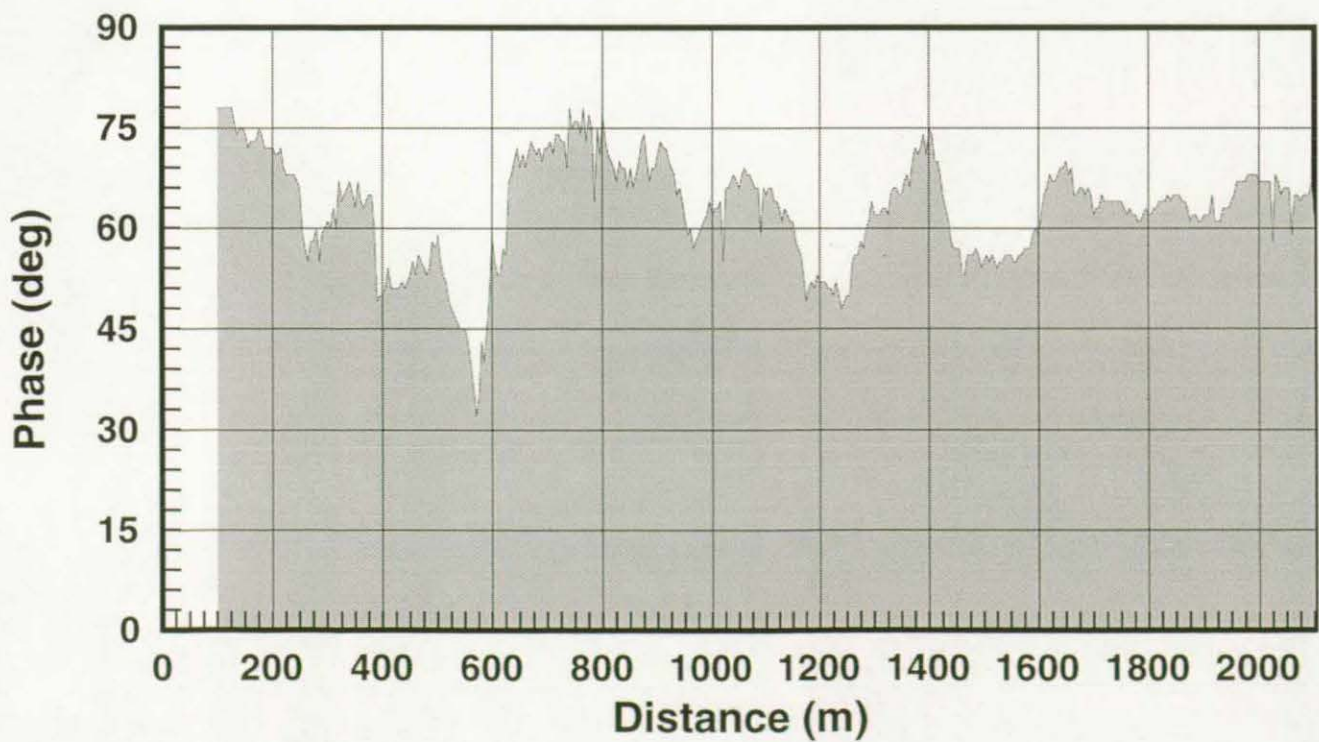


Fig. 4.3

**Xylophagu VLF survey 1998**

**18.3 kHz E-W 5m interval, 50 m LP**

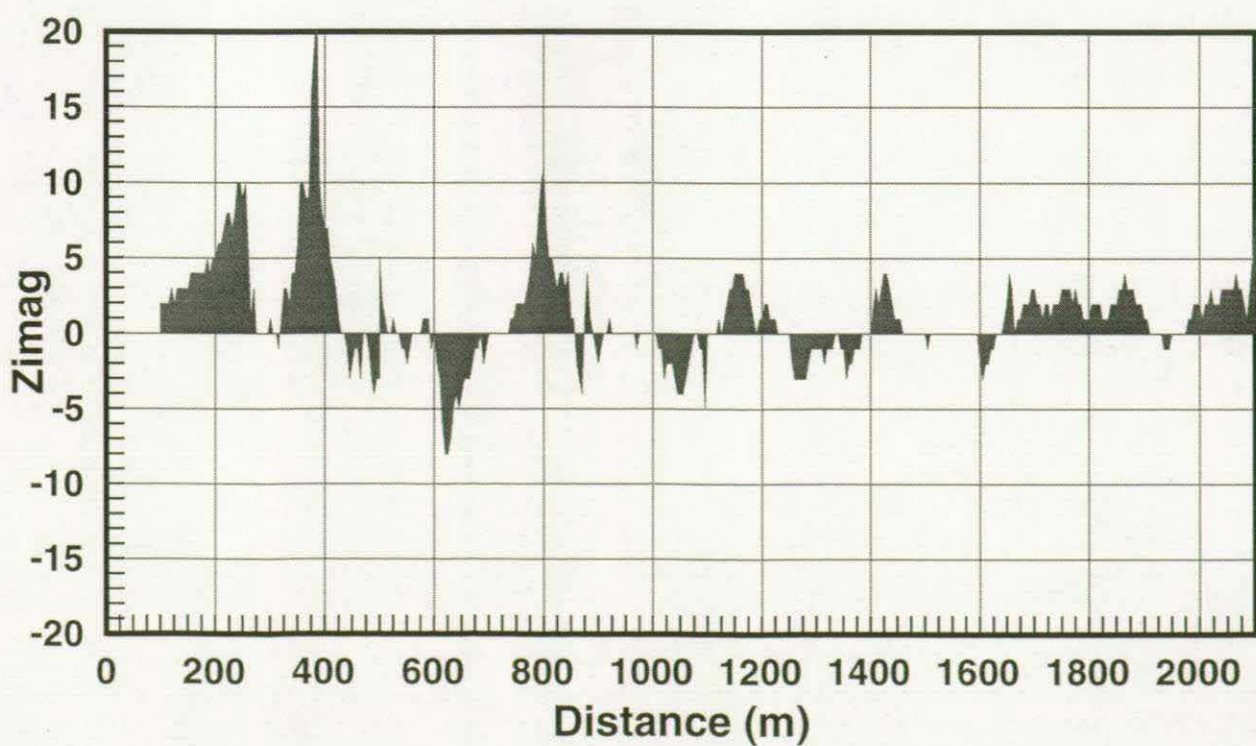
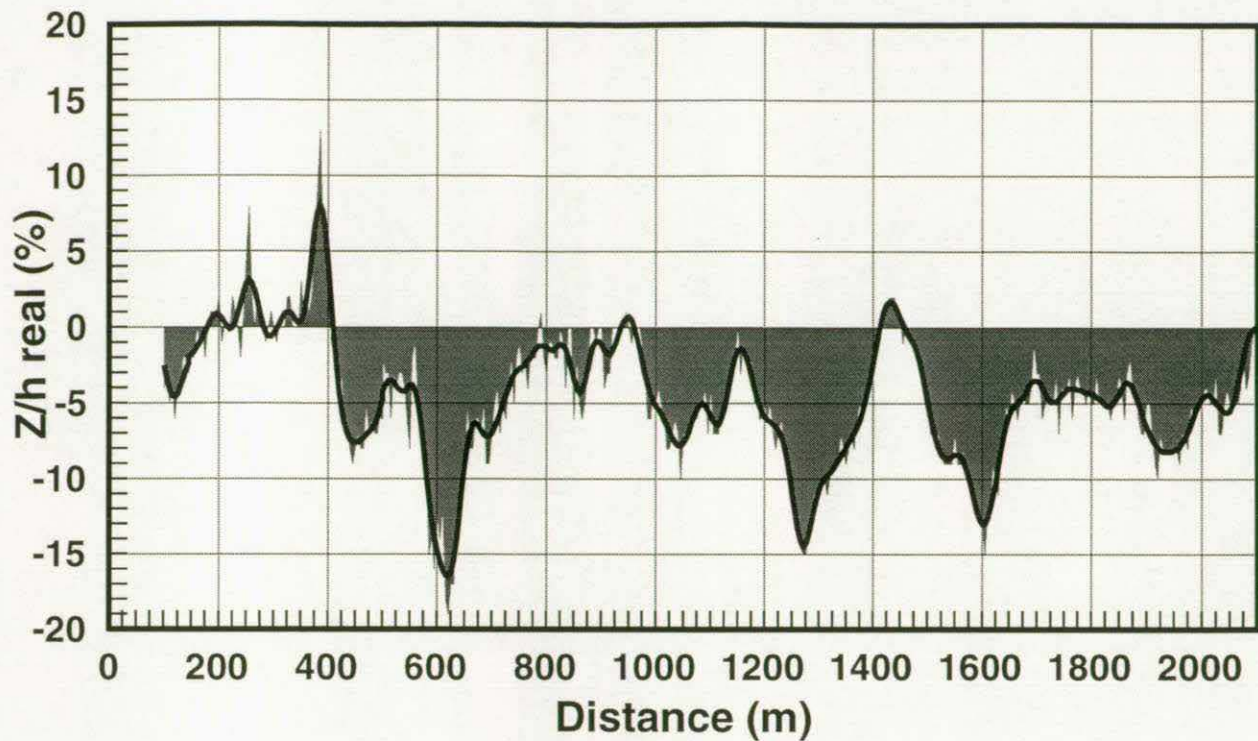
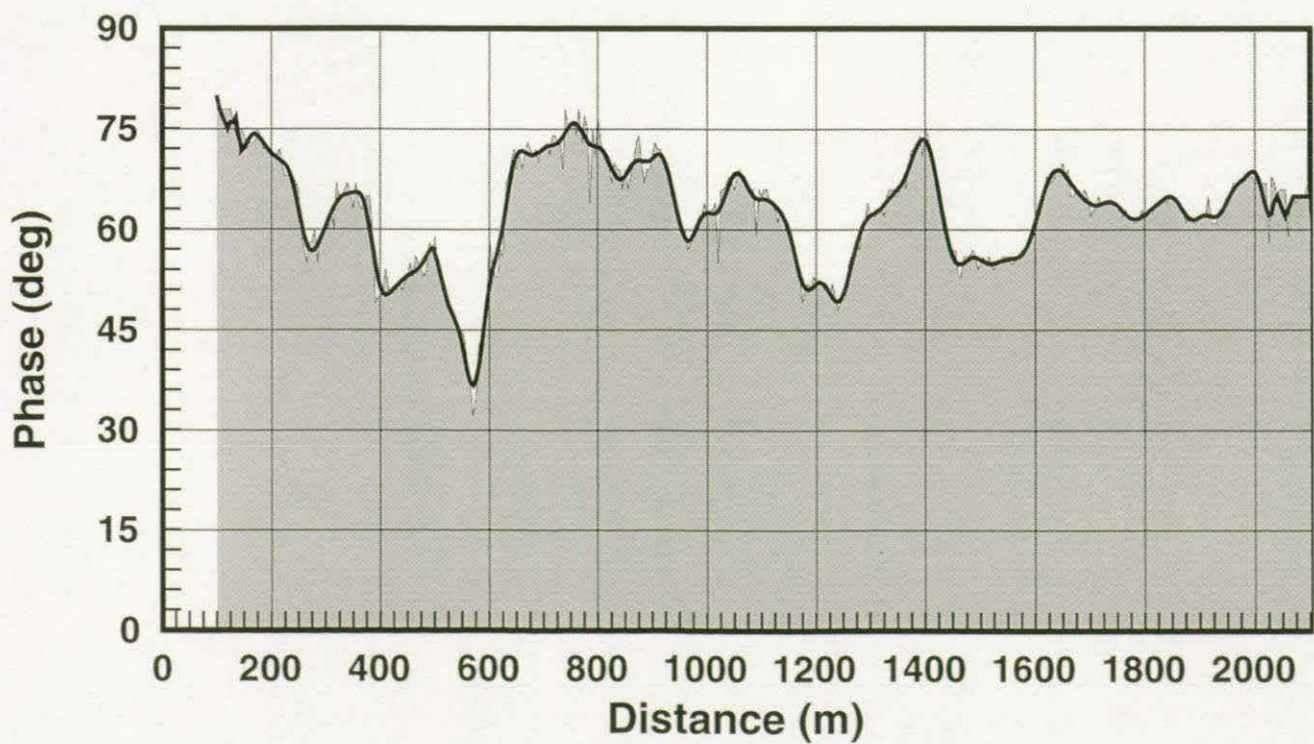
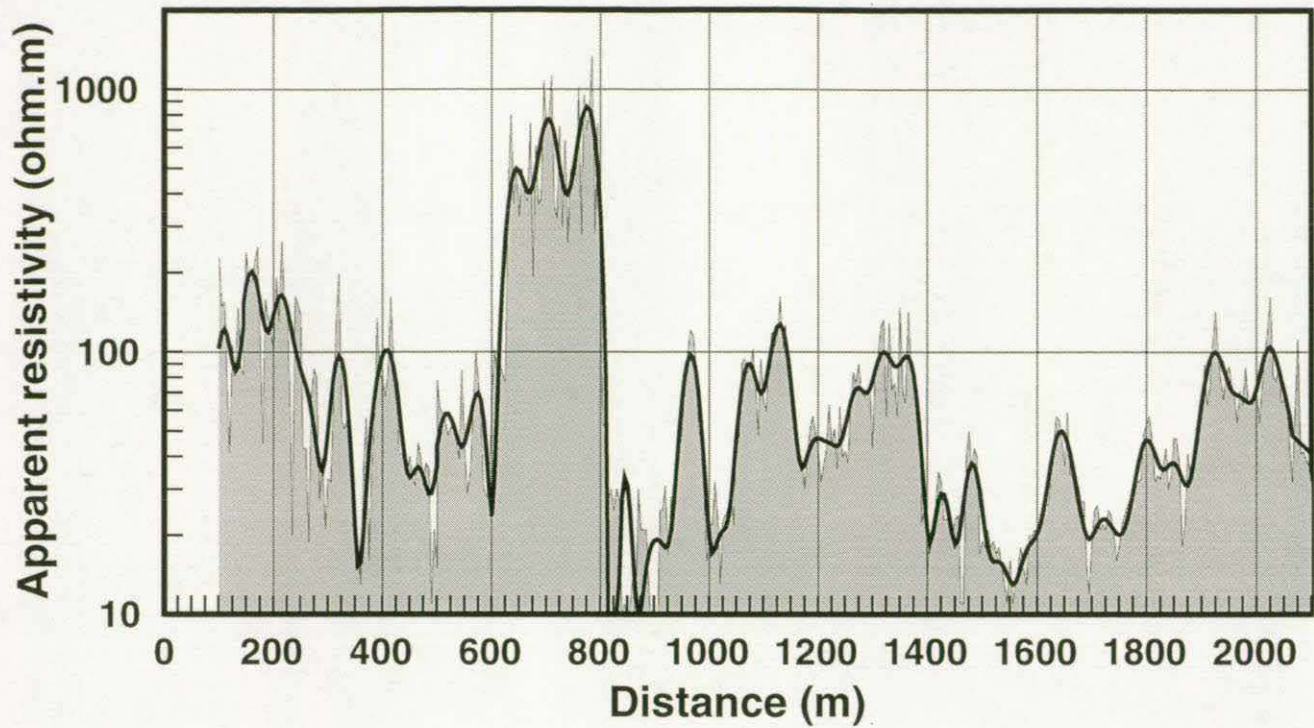


Fig. 4.4

**Xylophagu VLF survey 1998**

**18.3 kHz E-W 5m interval, 50 m LP**

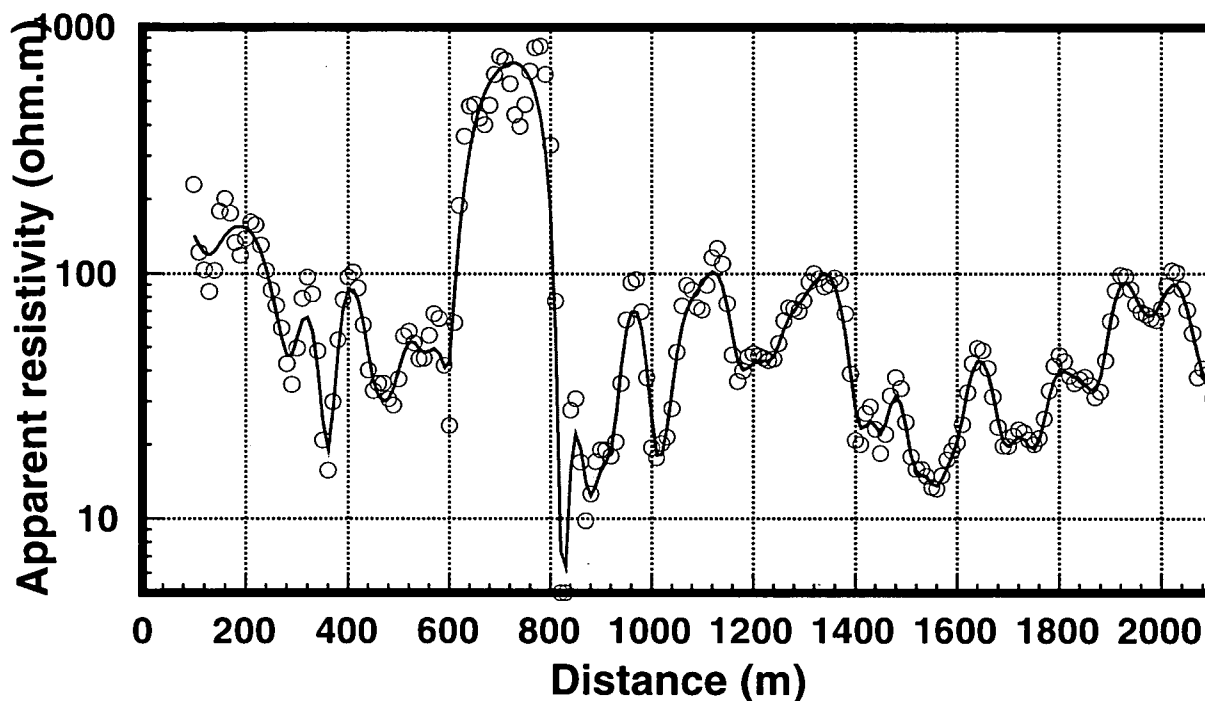


# Xylophagu VLF survey 1998

18.3 kHz E-W 10 m interval

Comparison of observed and modelled results

TE-mode. 2d NLCG. 10% data errors gives rms misfit of 1.5%



South

North

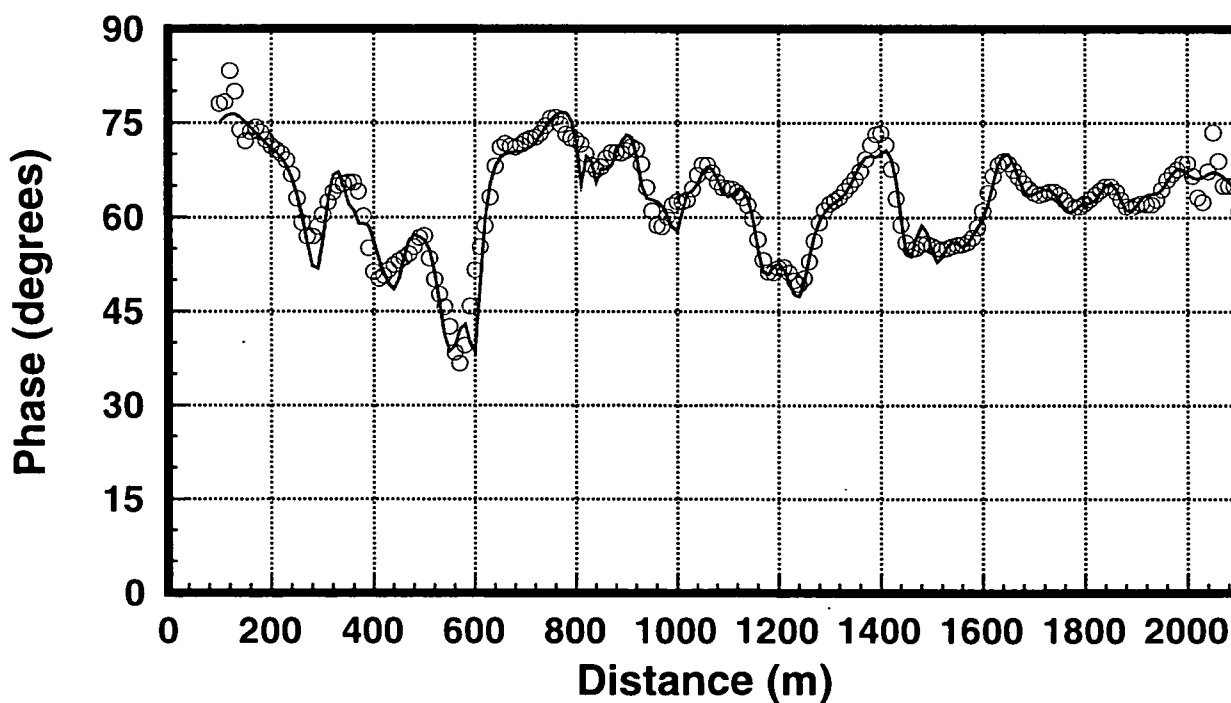
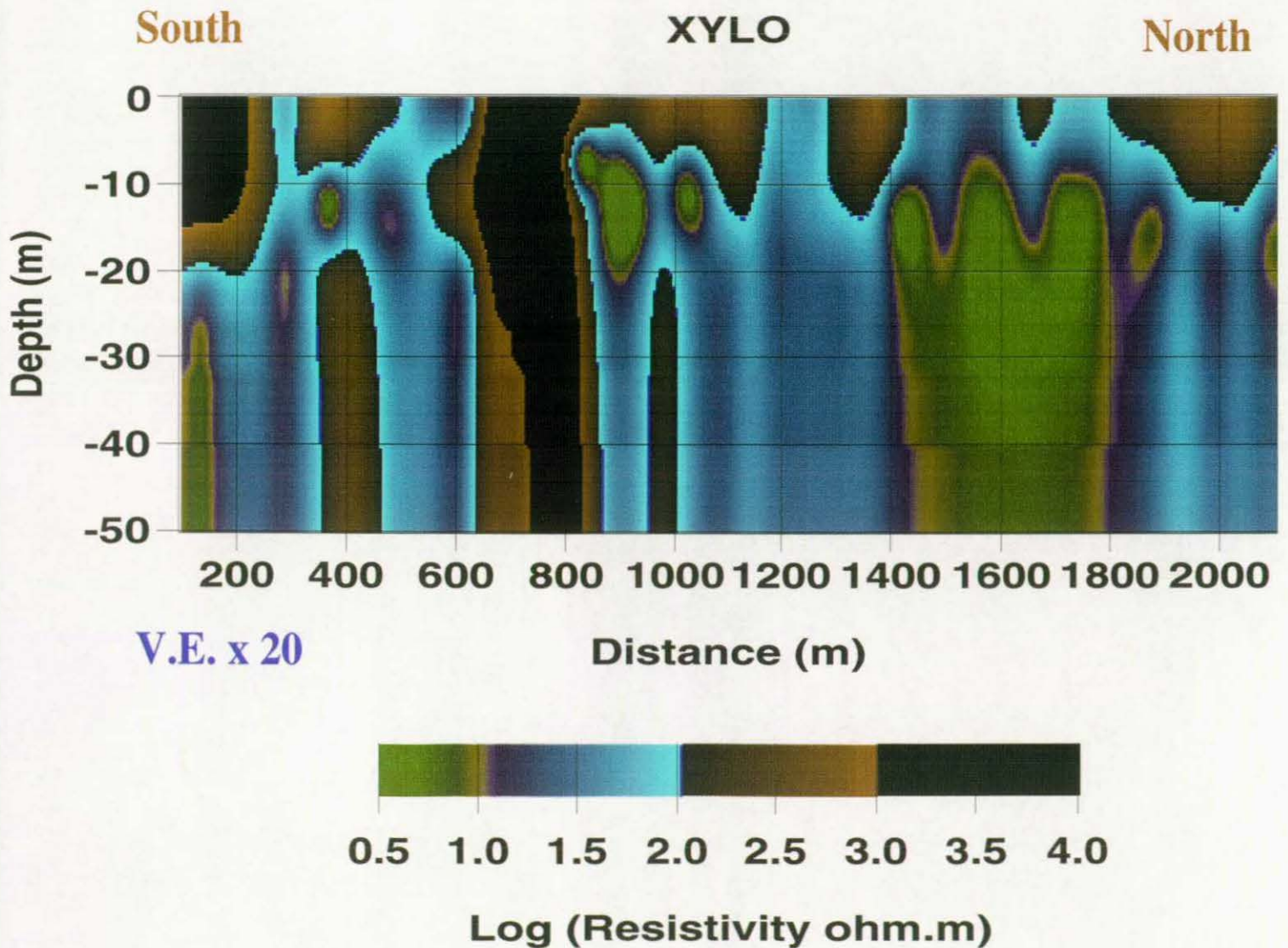


**Fig. 5.2**

**Cyprus VLF survey 98**

**Xylophagu 18.3 kHz TE**

**2D resistivity model using NLCG inversion**



TE-mode. 2d bNLCG. 10% data errors give misfit of 1.6%

Filtered data at 10 m, 201 observations of apparent resistivity and phase

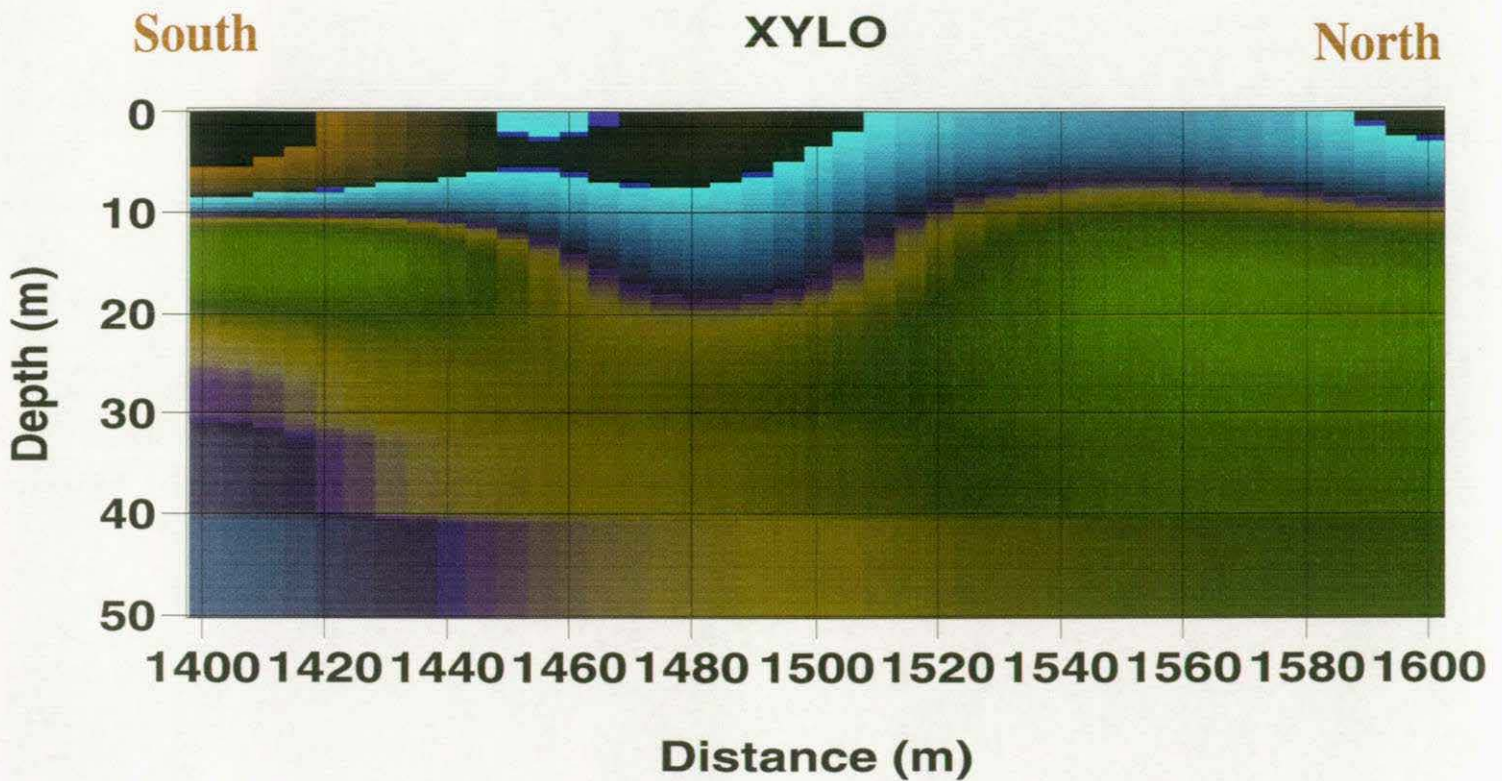
**Fig. 5.3**

**Cyprus VLF survey 98**

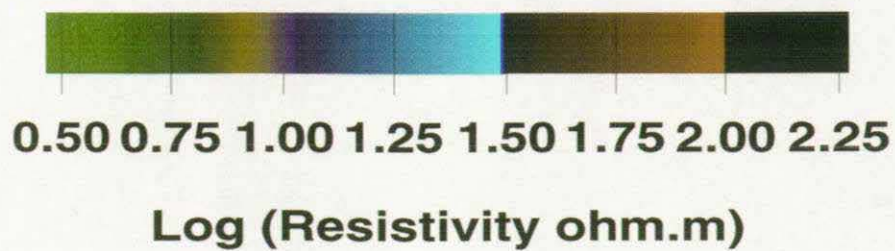
**Xylophagu 18.3 kHz TE**

**2D resistivity model using NLCG inversion**

**200 m detail from model**



**V.E. x 2**



TE-mode. 2d bNLCG. 10% data errors give misfit of 1.6%

Filtered data at 10 m, 201 observations of apparent resistivity and phase